Using Induced Pluripotent Stem Cells and Cardiomyocytes to Model the Splicing Defect in the LMNA Gene That Causes Hutchinson-Gilford Progeria

Using Induced Pluripotent Stem Cells and Cardiomyocytes to Model the Splicing Defect in the LMNA Gene that Causes Hutchinson-Gilford Progeria

Sarah A. Fahmy

A Thesis in the Field of Biology

for the Degree of Masters of Liberal Arts in Extension Studies

Harvard University

May 2017

Abstract

Hutchinson-Gilford Progeria syndrome (HGPS) is an extremely rare, fatal, autosomal dominant disease affecting roughly one in 18 million children (Ullrich *et al.* 2015). It is caused by a single base pair change in position 1824 resulting in a silent mutation (GGC > GGT) that causes a splicing defect in the LMNA gene. This resulting protein has a 50 amino acid deletion which is called progerin (Eriksson *et al.* 2003). Progeria is characterized by severe premature aging particularly affecting the skeletal-muscular system, the renal system, and the cardiovascular system. Patients with Hutchinson Gilford progeria typically live only an average of 14.6 years of age, dying from a heart attack or stroke resulting from hypertension and atherosclerosis (Ullrich *et al.* 2015).

The CRISPR (Clustered Regulatory Interspaced Short Palindromic Repeats) and associated Cas proteins originally found in *Streptococcus pyogenes* have been transformed into a revolutionary technology used in genome editing with long term hopes of therapeutic applications (Sander *et al.* 2014, Mali *et al.* 2015). Reprogramming somatic cells in to induced pluripotent stem cells is also an important tool in disease modeling (Yamanaka 2009).

This research aims to create a stem cell model of the Hutchinson-Gilford Progeria LMNA mutation with CRISPR Cas9 genome editing technology and iPS reprogramming, and to observe the phenotypes associated with the G608G mutation in differentiated

cardiac cells. This type of research allows for a better understanding of the pathology of the disease and provides insight as to which cell types are most affected. The goals of this research were three fold. First, to use CRISPR Cas9 tools and iPSC reprogramming to create an iPS line with the G608G in the LMNA gene. The second to differentiate the HGPS iPS cells generated from the first experiments into cardiomyocytes, and finally to evaluate the G608G phenotypes of cardiomyocytes and measure levels of metabolic markers indicative of hypertension caused by the G608G mutation, and the levels of progerin and LMNA expressed. In the future, these studies may be applied to research alternative stem cell therapies for humans with the progeria disease and in addition may provide greater insight to the pathology of atherosclerosis and the process of aging.

Dedication

This work is dedicated to Sam Berns, and to his parents, Drs. Leslie Gordon and Scott Berns. Sam was an extraordinary young man who inspired many with his bright, positive outlook on life. Despite being afflicted with Hutchinson-Gilford Progeria Syndrome, Sam was able to help the public understand life with the disease. I hope that the research I have been able to complete provides insight in to the ongoing battle to find a cure for HGPS.

Acknowledgments

This work would not have been made possible if it were not for many people. First, I would like to thank Dr. Laurence Daheron and Dr. Chad Cowan, my thesis directors. Laurence, thank you for fueling my passion for this research and always being there to talk about whatever I needed to talk about, whether related to this work or not. Thank you for your encouragement and support, especially when times were tough.

Second, I would like to thank Benjamín Erranz, who first started as just a visiting researcher from Chile but turned into a lifelong friend. Benjamín, I always say I do not know what I would do without you, and certainly it would not be being able to finish my work. Thank you for supporting me, and teaching me, but most of all for being a great support system and turning any situation into one that is full of laughs. I would also like to recognize the other members of the Harvard iPS Core Facility who have helped me along the way, no matter what. I couldn't have completed any of this without you all!

I would like to thank Thermo Fisher Scientific for providing me with the funding for my research, as well as my advisor, Dr. James Morris, for being a solid mentor not only during the course of my Master's degree, but during my undergraduate career as well.

Lastly, I would like to thank my family. To my mom and dad (Deani and Amr) for always providing me with a support system at home, and for helping with experiments, and my sister, Amina and brother, Youssef for always making me laugh.

Table of Contents

List of Tables

List of Figures

Chapter I. Introduction

Hutchinson-Gilford Progeria

Hutchinson Gilford Progeria syndrome (HGPS) is an extremely rare rapid premature aging disease seen in children caused by a single base pair mutation in the LMNA gene (Ullrich et al. 2015). This mutation induces a splicing defect that causes a 50 amino acid deletion on the C-terminal end of the protein resulting in the production of the protein progerin (levels of which can predict the severity of the disease). LMNA is usually located on the nuclear membrane. The mutant form leads to the removal of the proteolytic cleavage site of the farnesyl group (Ulrich *et al*. 2015). The hydrophobic character of the farnesyl group causes proteins to be membrane associated. When de-farnesylation cannot take place, progerin builds up along the nuclear membrane, causing nuclear blebbing (Figure 1). The nuclear blebbing in certain cell types causes severe premature aging, particularly in the skeletal muscular system, the renal system, and the cardiovascular system. Patients with Hutchinson Gilford progeria typically live only an average of 14.6 years of age, dying from a heart attack or stroke resulting from hypertension and atherosclerosis (Ulrich *et al.* 2015).

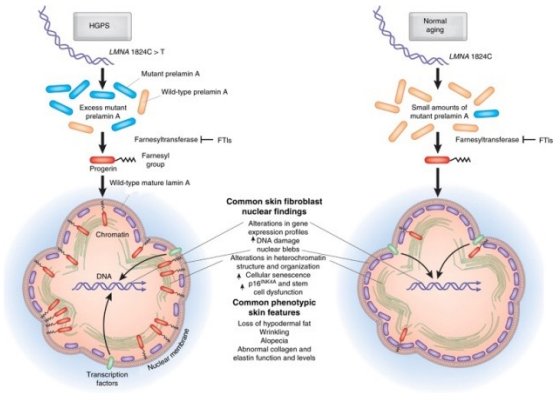

Figure 1: Nuclear behavior in HGPS and wild type patient fibroblasts (Capell *et al.* 2009).

Currently, there is no cure for the disease and only limited treatments for this disease exist. Farnesyltransferase inhibitors such as Lonafarnib have yielded positive results, but only for a couple of years after the start of the drug's administration (Ullrich *et al.* 2015, Wong *et al.* 2012). Other drugs such as Aspirin and statins which help reduce hypercholesterolemia and hypertension are also administered to reduce the risk of heart attack and stroke. Rapamycin has also been administered to decrease nuclear blebbing and improve cellular phenotypes (Ullrich *et al.* 2015).

The lack of defarnesylation of the progerin resulting from the G608G mutation in the LMNA gene has been the primary target of drug development for Progeria patients. Hypercholesterolemia and hypertension leading to severe atherosclerosis are two of the main symptoms that if successfully targeted, have the potential to increase the lifespan and quality of life of patients with HGPS.

Genome Editing & CRISPR

Genome editing in mammalian cells has opened the doors of major achievements in the fields of disease models and personalized medicine. There are three recent methods that facilitate the process of gene editing: zinc finger nucleases (ZFNs), transcription like effector nucleases (TALENS), and clustered regulatory interspaced short palindromic repeats (CRISPR) (Gaj *et al*. 2013). Zinc finger nucleases combine the nuclease activity of the FokI restriction enzyme and the DNA binding properties of zinc finger proteins. Two separate zinc fingers will bind to a target sequence inducing dimerization of the Fok1 enzyme, resulting in a double strand break in the DNA (Urnov *et al* 2010). Not long

after ZFNs became popular for genome editing, transcription like effector nucleases (TALENS) came in to the picture. TALENS are quite similar to ZFNs, they also consist of a non-specific FokI nuclease and a customizable DNA binding domain composed of transcription activator-like effectors secreted by the plant eating bacteria *Xanthomonas* (Joung *et al.* 2013).

Perhaps the most widely used method of genome editing is the CRISPR Cas9 system. The CRISPR-associated protein 9 nuclease is part of the adaptive immune machinery of the bacteria *Streptococcus pyogenes*. Clustered regulatory interspaced short palindromic sequences are loci that consist of short sequences that include sequences of viral or plasmid origin, so that when the bacteria is infected by a viral bacteriophage, for example, it is able to recognize that it is a foreign invader and prevent an infection (Marraffini 2016). The bacteria's Cas9 nuclease first cuts the target sequence upstream of a known sequence following the -NGG pattern, the protospacer adjacent motif (PAM). Following cleavage and excision of the foreign DNA sequence, endogenous DNA repair mechanisms then take over to re-ligate the DNA after cutting. The most common repair mechanism is non-homologous end joining, but it is error prone. Small, imprecise insertions or deletions are introduced at the site of the double stranded break. Another mechanism is homology directed repair. It requires the delivery of a DNA template, allowing the introduction of a precise point

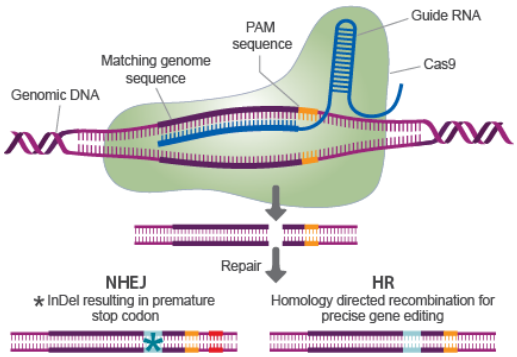

Figure 2: The CRISPR Cas9 cutting and repair mechanism (TRANSEdit 2015).

mutation or longer insertions by homologous recombination (Sander *et al.* 2014). These experiments hope to use homology directed repair to create a precise edit in the DNA sequence of the LMNA gene. The power of this bacterial enzymatic system has now been harnessed to edit the genome of mammalian cells. It was first introduced in to HEK293T cells, and can be virtually used in any cell type, including ES and iPS cells (Sander *et al.* 2014).

Although there are many uses that can come from genome editing, the field is also accompanied by a myriad of limitations and ethical considerations. Regardless of the method used, there is the chance that there will be undesired, off target cleavage events. Furthermore, there is a chance of low nuclease activity, and the likelihood of homology directed repair taking place is low compared to non-homologous end joining (Vasiliou *et al.* 2016). As genome editing technology develops, scientists are beginning to think about the consequences and implications of genome editing in human embryos, and how to regulate germ line editing. The experiments performed as part of this project make use of CRISPR Cas9 genome editing technology in human induced pluripotent stem cells.

Stem Cell Reprogramming

In 2006, Shinya Yamanaka changed the world when he discovered that somatic cells could be reprogrammed back in to a pluripotent state, similar to the state of embryonic stem cells in a simple and robust way. Upon retroviral introduction of four transcription factors, Oct3/4, Sox2, Klf4, and c-Myc, cell types such as fibroblasts could return to an undifferentiated, pluripotent state (Takahasi *et al.* 2006). Since the discovery

of these reprogramming factors, there have been different delivery techniques developed to approach reprogramming—namely using Sendai virus (SeV), Episomal vector, Lenti Virus, and via mRNA transfection (Schlaeger *et al.* 2015). For these experiments, the Sendai virus method and a non-modified RNA method were used for reprogramming. Cells that are designated to be pluripotent exhibit the same morphology as compared to ES cells, express certain genes specific to ES cells, and have the potential to differentiate in to the three germ layers, ectoderm, mesoderm, and endoderm (Takahashi *et al.* 2006). Different steps have been taken to ensure that the iPS cells are left without a trace of the transgenes and to reduce risks of oncogenesis (Eguchi *et al.* 2016).

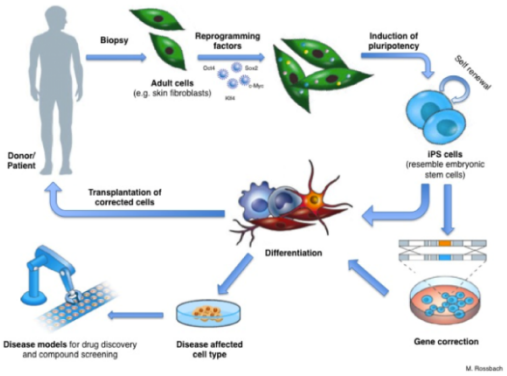

Figure 3: Overall step by step process of iPS cell reprogramming, editing, and differentiation (Rossbach 2012).

One of the most widespread methods is the Sendai virus because of its low pathogenicity, its capacity for high gene expression, and its ability to transduce a large number of cells in a myriad of different host organisms (Nakanisi *et al.* 2012). Furthermore, the SeV vector is able to express the reprogramming factors without integrating itself in to the host genome, and complete elimination of transgenes may be facilitated by the presence of a temperature sensitive mutation in the SeV containing c-Myc (Nakanisi *et al.* 2012).

Traditional mRNA transfection methods are accompanied by severe toxicity to the cell, as well as inhibition of mRNA translation (Stemgent). A new protocol has emerged to help evade these problems. This protocol uses a cocktail of different RNAs that is made up of non-modified reprogramming mRNAs of the traditional Yamanaka factors, immune evasion mRNAs, and microRNAs to enhance the reprogramming process (Poleganov *et al.* 2015). While traditional mRNA transfection methods of reprogramming are generally used to reprogram fibroblasts, and do not work for blood cells, this method has been optimized to reprogram endothelial progenitor cells derived from blood, and epithelial cells isolated from urine (Poleganov *et al.* 2015).

The ability to have cells with pluripotent capacity to rival that of ES cells has been a game changer for the field of cell therapy (Hotta *et al.* 2015). These cells have the ability to differentiate into different germ layers, providing an unlimited number of cells for transplantation, and potential immune rejection can be prevented by using autologous cells (Nakanisi *et al.* 2012). Induced pluripotent stem cells were derived from HGPS fibroblasts using a retroviral method. Interestingly, it was found that the iPS cells no longer express progerin, the abnormal protein produced by HGPS patients, and that the presence of nuclear blebbing diminished (Liu *et al.* 2011).

Cardiomyocyte Differentiation

Adult cardiomyocytes are non-proliferative, making them a difficult target in gene and cell therapy. Because cardiac disease is the leading cause of death in many countries, it is of interest to generate cardiac cells and develop models for these diseases (Batalov *et*

al. 2015). Cardiomyocytes were first derived in 2001 from human embryonic stem cells. ES cells were maintained in suspension and were allowed to form embryoid bodies (Kehat *et al.* 2001). The derived cells had the structural and functional properties of cardiomyocytes. However, this method has proven to be extremely inefficient, generating only 1% cardiomyocytes in the resulting cell population, and showing inconsistent differentiation potential across different iPS and ES cell lines (Lian *et al.* 2013). Both the Wnt/β-catenin pathway and the Gsk transcription pathway are highly involved in cardiogenesis (Tzahor 2007, Ishikawa *et al.*. 2012).

A more targeted approach to obtain cardiomyocyte takes advantage of chemically altering different developmental pathways, like the ones mentioned above. Currently, manipulation of the Wnt signaling pathway and application of Gsk3 inhibitors allow for a highly efficient differentiation process, yielding a nearly pure population of cardiomyocytes (Lian *et al.* 2013). Methods such as FACS analysis, qRT-PCR, and immunohistochemistry are effective methods to characterize the efficiency of the differentiation process (Bhattacharya *et al.* 2014). Premature cardiac aging has been observed in stem cell obtained from patients with an R225X mutation in exon 4 of the lamin A/C gene (Siu *et al*. 2012). Although this is not the classical mutation seen in progeria patients, it gives some insight as to how cardiac cells may age over time. This research aims to create cardiomyocytes directly from a HGPS patient exhibiting the classical G608G mutation.

Specific Aims & Hypotheses

Aim 1: a) Using a CRISPR system, create iPS cell lines containing the G608G progeria mutation.

b) Using Sendai virus and non-modified RNA transfection, fibroblasts from a progeria patient will be reprogrammed to induced pluripotent stem cells.

Hypotheses: a) Using a CRISPR-Cas9 system, LMNA knock-in iPS cells will be generated and confirmed.

b) Alternatively, using Sendai virus and non-modified RNA transfection, fibroblasts will be reprogrammed in to iPS cells.

Creating a stem cell line representative of a patient's cells will allow us to study the effects of the G608G mutation without involving a patient. Furthermore, using stem cells will allow us to generate different cell types after the mutation is confirmed. Induced pluripotent stem cells will be targeted using the CRISPR Cas9 system. Targeted cells will be screened for the G608G mutation, nuclear blebbing, and splicing will be confirmed using PCR and Western blot. Reprogramming HGPS fibroblasts will provide an alternative means to obtaining the disease modeled stem cells.

Aim 2: Using the mutant cells generated in Aim 1, cardiomyocytes will be derived.

Hypothesis: Using optimized differentiation protocols, G608G iPS cells will successfully be differentiated into cardiomyocytes.

Once the iPS cells containing the G608G mutation are confirmed, they will be differentiated into cardiomyocytes. Expression of cardiomyocyte markers will be

evaluated using FACS, qRT-PCR, and ICC to ensure differentiation was successful and to assess the differentiation efficiency. Successfully differentiated cells will be used in aim three to study the nuclear blebbing phenotype *in vitro,* and further study any transcriptional abnormalities associated with the disease.

Aim 3: Perform screening experiments to determine if mutant cardiomyocytes express a phenotype indicative of the G608G mutation and measure transcriptional functionality in these mutant lines.

Hypothesis: Derived HGPS cardiomyocyte mutants will show evidence of nuclear blebbing in culture, irregular gene expression indicative of hypertension, and elevated levels of LMNA and progerin.

Cardiomyocytes obtained from Aim 2 will be used to measure levels of brain naturietic peptide (BNP) to help understand how affected cardiomyocytes are contributing to hypertension. LMNA and progerin levels will also be observed in these cardiomyocytes. Furthermore, reprogrammed HGPS and BJ iPSCs will be differentiated into the three germ layers and levels of progerin will be observed in each lineage population. Changes in overall differentiation potential will be also be observed.

Definition of Terms

“Action Potential”: The change of electrical potential along the membrane of a muscle or nerve cell.

“Angiotensin”: Protein that promotes aldosterone secretion and causes an increase in blood pressure.

“Atherosclerosis”: Condition caused by a build up of cholesterol in the arteries that can cause heart attack and stroke.

“BNP”: Secreted by the ventricles of the heart in response to stretching of cardiomyocytes. Elevated in hypertensive patients.

“Calcium Channels”: Cellular membrane channel selective to calcium that causes action potential allowing the heart to contract.

“Cardiomyocytes”: Cardiac muscle cells.

“Cas9”: Protein used in conjunction with RNA guides to induce double stranded breaks in DNA.

“Clustered Regulatory Interspaced Short Palindromic Repeats (CRISPR)”: Short segments of DNA complimentary to an endogenous DNA sequence.

“Depolarization”: Loss of the difference of electric charge between the outside and inside of the cell membrane that results in a contraction

“Differentiation”: Process in which stem cells are turned into mature and specialized cells.

“Ectoderm”: Outermost layer of cells during development that eventually turn in to the epidermis and neural cell types.

“EKB-NM-RNA”: Reduces the cellular interferon response to exogenous mRNA. Added during NM-RNA reprogramming cocktail to enhance reprogramming efficiency and prevent cellular apoptosis.

“Embryonic Stem Cells (ESCs)”: Pluripotent stem cells derived from a pre-implantation embryo.

“Endoderm”: Innermost layer of cells during development that eventually turn into the lining of the gut and other associated cell types.

“Fluorescence Activated Cell Sorting (FACS)”: Specialized type of flow cytometry that uses the presence of a fluorescence protein that identifies a small population of cells.

“Fura-2”: Indicator of intracellular calcium levels.

“G608G”: Silent mutation on the LMNA gene resulting in a RNA splicing defect causing a 50 base pair deletion that is responsible for progeria.

“Green Fluorescent Protein (GFP)”: Protein that glows green when exposed to light in the blue to ultraviolet range

“High Density Lipoprotein (HDL)”: Lipoprotein high in protein to lipid ratio. “Good” cholesterol.

“Homology Directed Repair”: Endogenous mechanism employed by cells to repair double stranded breaks

“Hypertension”: High blood pressure that happens when the force of the flow of blood against artery walls is too high.

“Hutchinson Gilford Progeria Syndrome (HGPS)”: Rare premature aging disease- subject of this study.

“Hydrophobic”: A non-polar chemical species that preferentially interacts with other non-polar species, and does not interact with polar ones.

“Immunocytochemistry (ICC)”: Method to assess the presence of proteins in cells.

“Induced Pluripotent Stem Cells (iPSCs)”: Type of stem cell that are directly reprogrammed from specialized adult cells such as fibroblasts or blood cells.

“Low Density Lipoprotein (LDL)”: Lipoprotein with low protein to lipid ratio. “Bad” cholesterol.

“Murine embryonic fibroblasts (MEF)”: Fibroblasts derived from early stage embryo of a mouse- used as feeder to assist with stem cell adhesion and maintenance.

“Mesendoderm”: Embryonic tissue layer with the potential to differentiate into either mesoderm or endoderm.

“Mesoderm”: The middle layer of cells in an embryo during development that will eventually differentiate into muscle cells and other associated cell types.

“NM-RNA”: RNA that performs *in vitro* transcription using normal nucleosides.

“LMNA”: Nuclear membrane protein in which point mutation causing progeria is found.

“Lonafarnib”: Farnesyltransferase inhibitor that is being used as a drug to treat symptoms of progeria.

“NM-microRNAs”: Enhances efficiency of RNA based reprogramming methods.

“Nuclear Blebbing”: Phenotype associated with progeria. Protrusion of the nuclear membrane that degrades the interior of the nucleus.

“OKSMNL NM-RNA”: Mixture of mRNAs encoding for Ocr4, Sox2, Klf4, cMyc, Nanog, and Lin28.

“Polymerase Chain Reaction (PCR)”: Technique used to amplify a specific portion of DNA.

“Progenitor Cells”: A cell that can differentiate into different, more specialized cells.

“Protospacer adjacent motif (PAM)”: Sequence in the form of NGG that the CRISPR Cas9 complex recognizes and binds to.

“Progerin”: Protein produced as a result of the G608G mutation on the LMNA gene. Levels of this protein can predict the severity of the disease phenotypes.

“Quantitative Real Time PCR (qPCR)”: Method used to measure levels of RNA in cells to quantify levels of transcription.

“Rapamycin”: Immunosuppressant used as an anti-aging drug.

“Reprogramming”: Method in which specialized adult cells are reverted to the pluripotent embryonic like state.

“Sanger Sequencing”: Method of DNA sequencing.

“Sendai Virus”: Virus that primarily affects respiratory tract of rodents. Used for high capacity transduction in human cells *in vitro.*

“Single Stranded Donor Oligonucleotide (ssODN)”: Short piece of DNA used as a donor sequence containing a target site for incorporation using genome editing.

“SIRPA”: Signal regulatory protein alpha, transmembrane protein that negatively regulates tyrosine kinase coupled signaling.

“Splicing”: Editing of RNA sequence that removes introns and joins exons together. Splicing mechanism is disrupted in progeria.

“Transfection”: Process of introducing exogenous genetic material into cells that makes use of the cells own machinery.“TGF-β Pathway”: Signaling pathway involved in cell growth, cell differentiation, apoptosis, and other cellular functions.

“TNNT2”: Cardiac troponin 2, regulate cardiomyocyte contraction in response to intracellular calcium levels.

“Wnt Signaling Pathway”: Cell signal transduction pathway involved in cell fate specification, body axis patterning, proliferation, and migration during embryogenesis.

Chapter II. Materials & Methods

Genome Editing

CRISPR Design & Testing

Guide RNA Design | The LMNA sequence was obtained from the National Institute of Health (NIH) database, and Geneious software was used to identify the single nucleotide in position 1824 in the LMNA gene where the mutation causing HGPS is located. Guide RNAs were designed *in silico* by inputting a 50 base pair sequence flanking position 1824 in to the MIT CRISPR design tool and the CRISPOR online tool (Hendriks *et a.* 2015 CRISPOR). Phosphorylated 5' end sense and antisense guide oligonucleotides were ordered from IDT, annealed, and ligated in to the pSPgRNA vector (Addgene) (Table 1).

Cloning and Plasmid Isolation | Annealed guides were transformed in to Top10 Competent *E. Coli* cells and plated on ampicillin resistance LB Agar plates and grown for 16 hours at 37^{o} Celsius. Single colonies were picked and inoculated in LB Amp media and grown overnight. Plasmid DNA was extracted using the miniprep kit by Qiagen as described according to the manufacturer, and DNA was sent for Sanger sequencing at Genewiz using the universal primers M13 Fwd(-21) and M13 Rev. Successful ligation of the guides were confirmed by comparing sequenced plasmids to the backbone sequence of the plasmid. Plasmids were maxi prepped using the endotoxin free Maxi prep kit by Qiagen as described by the manufacturer's protocol (Hendriks *et al.* 2015).

Guide RNA Cutting Efficiency | 24 hours prior to transfection, HEK 293T cells were plated at a density of 5 x 10^5 cells per well of an uncoated 6-well plate. Cells were maintained at 37^o Celsius in 5% CO_2 and fed every 24 hours with Dulbecco's Modified Eagle Medium (DMEM) supplemented with 10% fetal bovine serum and 1% penicillin/ streptomycin antibiotic cocktail. 1.2 µg of each purified guide along with a 1.6 µg of a plasmid containing both Cas9 and GFP were transfected in to the HEK293T cells using lipofectamine 2000. Cells were imaged 24 and 48 hours after transfection to evaluate transfection efficiency. 48 hours after transfection, cells were harvested using 0.05% Trypsin/EDTA and genomic DNA was extracted using the Qiagen. Primers that flank the region of nuclease activity were designed *in silico* using Primer3 Plus and subsequently ordered from IDT. Primer conditions were optimized by amplifying WT gDNA on a temperature gradient. The region of interest was amplified by PCR (Table 2) and run on a 2% agarose gel. PCR products were sent for Sanger sequencing using the forward and reverse primers used in PCR. Nuclease activity was measured *in silico* using the TIDE online analysis tool. A 125 basepair single stranded oligonucleotide was designed to incorporate the GGC > GGT silent mutation at position 1824 in the LMNA gene and ordered desalted at the 4nm scale from IDT.

hiPSC Knockin

Genome Editing iPS Culture & Transfection | The induced pluripotent stem cell (iPSC) line used for genome editing, BJ SiPS-C, was derived by the Harvard iPS Core Facility from foreskin fibroblasts using the Sendai virus methods deliver the Yamanaka

factors at an MOI of 5-5-3 ((Klf4-Oct3/4-Sox2 Sendai virus, c-Myc Sendai virus and Klf4 Sendai virus) (Takahasi *et al.* 2006). Cells were maintained at 37° Celsius in 5% CO_2. BJ SiPS-C were cultured simultaneously in two conditions, on Matrigel fed with mTeSR1 medium, and on Geltrex fed with StemFlex medium. Cells were fed every 24 hours, and passaged 1:3 at 80% confluence using Gentle Cell Dissociation Reagent (approximately every four days).

Prior to transfection, cells were dissociated to single cell using diluted (1:3) accutase in PBS(-/-). Cells in both conditions were dissociated and a live cell count was taken using trypan blue. 1.2 µg Cas9GFP, 0.6 µg Guide RNA, and 1.2 µg of ssODN were transfected into 1 x 10^6 cells in suspension before being re-plated on to one well of a 6 well plate. 10 µM Y27632 (Rock Inhibitor) was added to the plating media to enhance cell attachment and survival, and 10 µM the L755-507 small molecule was added to enhance homology directed repair (Yu *et al.* 2015). Cells were fed and imaged every 24 hours and kept in culture for 48 hours after transfection.

48 hours post transfection, cells were dissociated using 1:3 Accutase in PBS, resuspended in cold PBS, and collected in a 35 µm found bottom filter tube. Using the BD Aria FACS machine, cells expressing GFP were sorted through a 100 µm nozzle into an eppendorf tube containing mTeSR1 or StemFlex media, 10µM Y27632 (Rock Inhibitor), and MycoZap, and subsequently plated on 10cm dishes at a density of 20,000 cells per plate in conditioned media containing bFGF. For each transfection condition, one cell per well of a 96 well plate were collected directly after sorting and cultured for a few days. Transfections and FACS procedures were repeated once.

Cells were kept in culture until visible, nickel sized colonies were seen at 10x. Individual colonies were picked using a dissection microscope and seeded into three 96 well plates per each culture condition. Cells were maintained until they reached an 85% confluence. They were then split 1:3 using 1:3 accutase in PBS. 1/3 of the cells were put back into culture, 1/3 were frozen in 2x freezing media (20% DMSO in FBS), and 1/3 were resuspended in PBS, and genomic DNA was extracted using the PrepGem DNA extraction kit by ZyGem. For each clone, the region of interest was amplified by PCR, run on a 1% agarose gel at 200V for 1.5 hours, and sent for PCR cleanup and Sanger sequencing. Sequences were analyzed *in silico* using Geneious software to see if the ssODN containing the G608G (GGC > GGT) mutation was successfully taken up by the cells.

iPSC Reprogramming

Fibroblast Culture | Fibroblasts from a Progeria patient were obtained from Coriell cell repository (Catalog No: A30468). The fibroblasts originated from a 14 year old male who exhibited the classical form of Progeria, and had a confirmed G608G mutation in exon 11 of the LMNA gene. BJ foreskin fibroblasts were obtained from ATCC. At the start of culture, fibroblasts were tested for mycoplasma using the Lonza MycoAlert kit. Cells were cultured on MEF media consisting of DMEM supplemented with 10% FBS and 1% penicillin / streptomycin. Cells were passaged with 0.05% Trypsin / EDTA once they reached 85% confluence.

Sendai Virus Reprogramming | WT and HGPS fibroblasts were trypsinized and counted. 24 hours prior to transduction, 200,000 cells were plated onto 2 wells of a 6 well plated coated with 0.1% gelatin. On the day of the transduction, one well was harvested and counted to estimate the number of cells in the other well. The volume of virus needed was calculated based on the following formula:

$$\text{Volume of virus (ul)} = \frac{\text{MOI}\left(\frac{\text{CIU}}{\text{cell}}\right) x \ number\ of\ cells}{\text{titer of virus}\left(\frac{\text{CIU}}{\text{ml}}\right) x\ 10^{-3}}$$

The viral particles were transduced at the following MOIs:

KOS: MOI = 5 Myc: MOI = 5 KLF4: MOI = 3

Virus was transduced as described (ThermoFisher Cytotune 2.0). Cells were replaced in the incubator and fed 24 hours after transduction with fresh fibroblasts medium. Transduced cells were kept in culture for 6 days and fed every other day with fibroblast medium. Seven days after transduction, transduced cells were dissociated using 0.05% Trypsin/EDTA and plated on to 10 cm dishes seeded with MEF and fed with fibroblast medium. 24 hours later, cells were switched to hES medium consisting of DMEM, 20% KOSR, 1% L-Glutamine, 1% penicillin/streptomycin, 1% MEM-NEAA, and 0.1% 2-Mercaptoethanol supplemented with bFGF (10 ng/mL). Colonies were picked 28 days post transduction and seeded onto a 6 well plate coated with Matrigel. Upon picking, cells were switched to mTeSR1 medium.

Non-modified RNA Reprogramming | WT and HGPS fibroblasts were trypsinized and counted. 100,000 cells were plated on to one well of a 6 well plate and fed with fibroblast medium. 24 hours after plating, cells were transfected via RNA-iMax

with 1.8 µg of RNA as described (Stemgent). The NM-RNA reprogramming cocktail is composed of 0.8 µg OSKMNL NM-RNA, 0.6 µg EKB NM-RNA, and 0.4 µg NM-microRNAs (Stemgent). Upon transfection, the cells were switched from fibroblast media to Nutristem media. 15-18 hours after the first transfection, media was changed. The cells were transfected again 24 hours after the first transfection for a total of four days and four transfections. Colonies were picked ten days after transfection. The reprogramming process of the BJ fibroblasts was recorded every 6 hours using the CT-Biostation from Nikon.

Characterization | After reprogramming, cells were characterized by three methods- karyotype analysis, immunocytochemistry (ICC), and qRT-PCR to analyze pluripotency and differentiation potential.

Karyotype Analysis | Cells were seeded on to a T25 flask to a confluence of 60% and shipped to Wicell for karyotype analysis.

Immunocytochemistry | Cells were seeded on to a 48 well plate and fixed with 4% PFA and permeabilized with 0.1% Triton X-100 / PBS. Wash steps were carried out using 0.05% Tween 20 / PBS. Cells were blocked with 4% donkey serum in PBS. The following primary antibodies were diluted in 4% donkey serum and incubated overnight on the cells at 4^{o} C (Oct4 1:100 (ab19857), Nanog (ab21624) 1:50, SSEA3 (MAB4303), 1:200, SSEA4 (MAB 4304) 1:200, and TRA-1-60 (MAB4360) 1:200). Secondary antibodies (Anti-Mouse IgG (A21121), Anti-Mouse IgM (A21426), Anti-Rabbit (A21206), and Anti-Rat (A21213) were diluted 1:1000 in PBS and used to probe for the primary antibody. Cells were then stained with DAPI and imaged.

Reprogrammed iPSCs were harvested and resuspended in buffer RLT from the RNEasy RNA extraction by Qiagen. RNA was extracted as described by the manufacturer. A total of 1 µg of RNA was reversed transcribed to cDNA using the qScript cDNA SuperMix by Quanta. A 15 µL qRT-PCR reaction was carried out using 0.5µM taqman probes (RPLPO, Oct4, Lin28, and Sox2) (Table 3), 5µL of 1:20 diluted cDNA, and 10uL of Taqman Gene Expression Master Mix at a final concentration of 1x. Reactions were standardized to housekeeping genes and ΔΔCt was analyzed.

To analyze differentiation potential, reprogrammed iPSCs underwent directed differentiation using the STEMdiff Trilineage Differentiation Kit (Stemcell Technologies). 800,000 cells each were plated on two wells of a 12-well plate for ectoderm and endoderm differentiation, and 200,000 cells were plated on one well of a 12-well for mesoderm differentiation. For endoderm and mesoderm lineage differentiated cells, cells were fed with the respective medium for five days, while ectoderm lineage differentiated cells were fed for seven days. Cells were harvested, RNA was extracted and reverse transcribed to cDNA. A 10 µL qRT-PCR reaction was carried out using 0.5µM primers (Pax6, Brachyury, Sox17, and Actin) (Table 3), 2 µL of 1:20 diluted cDNA, and PerfeCTa SYBR Green FastMix Low Rox at a final concentration of 1x. Reactions were standardized to housekeeping genes and ΔΔCt was analyzed.

Aim 2: Cardiomyocyte Differentiation

Reprogrammed hiPSCs were dissociated to single cell using 1:3 accutase and seeded at a density of 500,000 cells per well of a 12-well Matrigel coated plate with

10uM rock inhibitor. Cells were fed every 24 hours for four days with 2mL of mTeSR1 per well. Four days after cells were seeded, differentiation to cardiomyocytes was induced (Day 0) by removing mTeSR1 media and feeding the cells with 2 mL of RPMI 1640 (+ Glutamine) containing B27 Supplement - Insulin and 12 μM of a Gsk3 inhibitor, in this case CHIR99021. 72 hours after induction, 2 mL of RPMI 1640 (+ Glutamine) containing B27 supplement - Insulin and 5 μM of the Wnt signaling inhibitor IWP2 was added. Media was changed 48 hours later with RMPI 1640 + B27-Insulin. 48 hours later, the media regimen was switched to RMPI 1640 + B27 supplement.This media was used for the remainder of the differentiation process and cells were fed every 48 hours. At day 7 post induction, cells were monitored under the microscope for the presence of beating cardiomyocytes, and monitored every day after that until beating was visualized.

To quantify the efficiency of the cardiomyocyte differentiation, immunocytochemistry was done on cardiomyocytes replated on a 48 well plate. The presence of NKX2.5 and TNNT2 was measured using the Human Cardiomyocyte Immunocytochemistry Kit as described (Thermo).

Differentiated cells were also analyzed by FACS to help quantify the efficiency (Burridge *et al.* 2015). Cells were analyzed based on the presence of cardiac troponin TNNT1 (intracellular) and analyzed/sorted based on the presence of SIRPA (surface). Cells were harvested and fixed with 4% PFA in PBS, permeabilized with Triton X-100, and stained with TNNT2 (Abcam 1:200), and SIRPA (Abcam 1:100). An AlexaFluor 488 goat anti-rabbit secondary antibody (1:1000) was used to select for TNNT2 and SIRPA. Cells were resuspended in 300 uL of cold 0.5% BSA/PBS, collected in a 35 μm round

bottom filter tube, and analyzed using the BD Aria FACS machine. Sorted cells were collected in a 1.5 mL eppendorf tube, and cells were isolated for RNA extraction.

To further analyze the cardiomyocyte differentiation efficiency, differentiated cells were harvested, RNA was extracted and reverse transcribed to cDNA. A 10 μL qPCR reaction was carried out using 0.5 μM primers (ACTC1, MYH7, NKX2.5, TNNT2, BNP, and Actin) (Table 3), 2 μL of 1:20 diluted cDNA, and PerfeCTa SYBR Green FastMix Low Rox at a final concentration of 1x. Reactions were standardized to housekeeping genes and ΔΔCt was analyzed.

Aim 3: Analysis of HGPS Cell Lines

RNA was extracted from reprogrammed iPSCs differentiated directly into the three germ layers using the RNeasy RNA Extraction kit by Qiagen. A total of 1 μg of RNA was reversed transcribed to cDNA using the qScript cDNA SuperMix by Quanta. A 25 μL RT-PCR was set up using 2 μL of 1:20 diluted cDNA and Taq DNA polymerase, and10 μM primers specific to areas of Exon 9 and Exon 12 of the LMNA gene. The presence of a single band at 510 bp indicates an in tact LMNA transcript, and the presence of two bands, one at 510 bp and one at 360 bp gives evidence that the truncated form of LMNA, progerin, is being transcribed. RT-PCR products were run through a 2.0% TBE agarose gel and analyzed for the presence of two bands (Scaffidi *et al.* 2006).

Chapter III. Results

Aim 1a

CRISPR Design & Testing

Geneious was used to identify the site of the G608G mutation in the LMNA gene (Figure S1). The MIT CRISPR design and CRISPOR online design tools were used to generate gRNA sequences in close proximity to mutation site (Table 3). Guides with off target scores lower than 60 were not taken into consideration for this project. Higher off target scores indicate that the guide RNA is more likely to cut at a specific locus, rather than in an unwanted location. HEK 293T cells were transfected with purified guide RNA and a conjugated Cas9GFP plasmid (Figure 4). The transfected HEK 293T cells transfected with each guide exhibited clear uptake of the Cas9GFP indicating that the transfection was successful.

Figure 4:

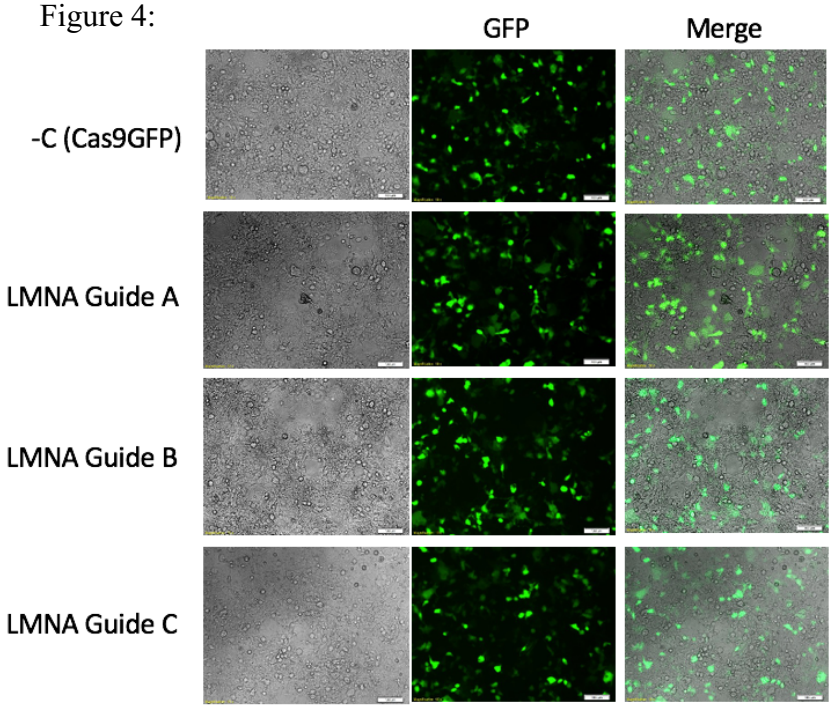

Figure 4: HEK293T cells were transfected with each RNA guide and the Cas9GFP plasmid. Presence of GFP indicates that the transfection was successful. Transfection efficiency was not altered and remained high with the addition of guide RNAs.

Cells were harvested after 48 hours and the region of interest was amplified by PCR, run on a 2% agarose gel, and sent for Sanger sequencing (Figure 5). Previously, separate primer pairs were tested on a temperature gradient to determine ideal PCR conditions (Figure S2). The 526 base pair region of interest was successfully amplified in a wild type control, in all 6 samples transfected with guide RNAs, and in fibroblasts from a patient exhibiting progeria.

Figure 5:

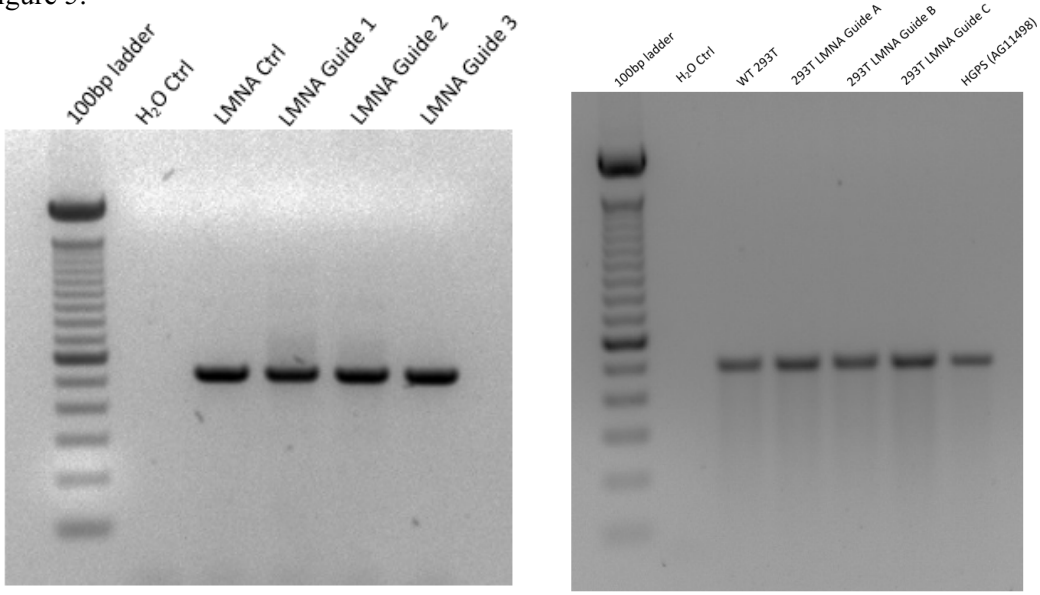

Figure 5: Primers flanking the site of the HGPS mutation were used to amplify gDNA extracted from transfected HEK 293T cells. A 526 base pair product indicates a successful amplification.

Quantification of nuclease activity was performed using the TIDE online tool. LMNA Guide 1 (Figure 6) cut at a 38.6% cutting efficiency, LMNA Guide 2 (Figure S4) at 28.8%, and LMNA Guide 3 (Figure S4) at 4.2% efficiency. Guides designed in round two showed substantially less cutting. LMNA Guide A cut at a 3.0 % efficiency (Figure S5),

Figure 6:

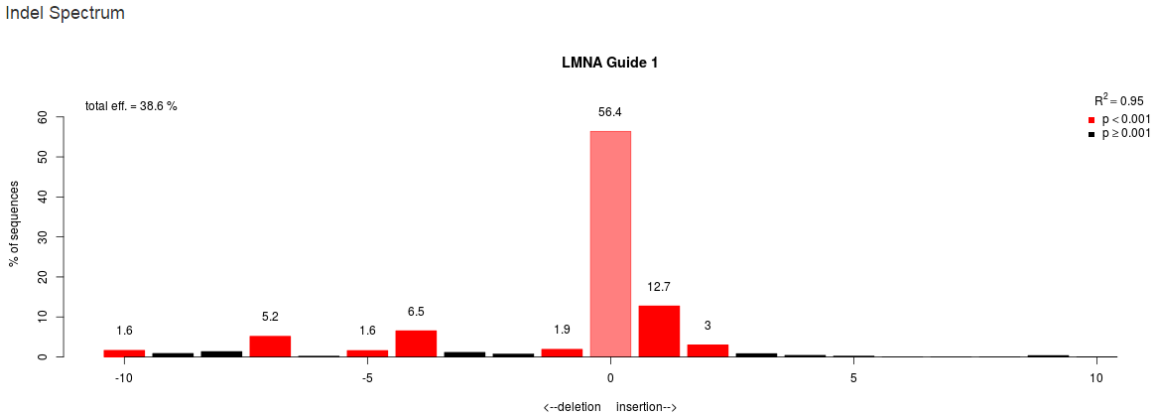

Figure 6: Sanger sequences of the uncut region of interest and the cut area of interest were compared. The tide online tool assesses mismatch in basepair peaks and area under the curve to quantify cutting efficiency in terms of insertions and deletions. LMNA Guide 1 performed at a 38.6% cutting efficiency, eliciting both insertion and deletion events around the cutting site of Guide 1.

LMNA Guide B at 3.3 % efficiency (Figure S5), and LMNA Guide C (Figure S5) at a 2.0 % efficiency. Based on TIDE results, LMNA Guide 1 was chosen for the knock-in experiment. A single oligonucleotide containing the G608G mutation responsible for HGPS was designed around the cutting site of LMNA Guide 1 (Table 3).

.

hiPSC Knock-in

BJ SiPS-C cells were cultured and maintained under two different conditions: on Matrigel fed with mTeSR1, and on Geltrex fed with StemFlex. Cells were imaged two days after passaging. In general, cells cultured in the Geltrex/StemFlex conditions looked healthier, and had a rounder, more ESC like morphology (Figure 7).

Figure 7:

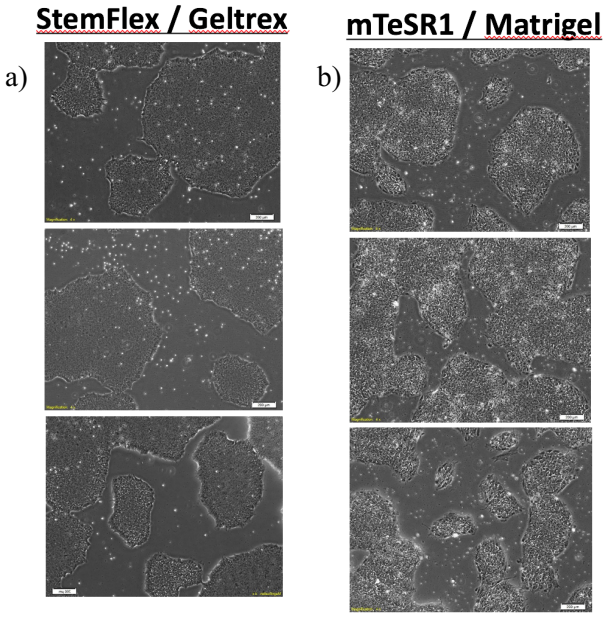

Figure 7: a) BJ SiPSCs cultured in StemFlex medium and Geltrex matrix exhibited a beautiful, compact, round morphology. Cells exhibited a healthier morphology after splitting. b) BJ SiPSCs cultured in mTeSR1 medium and Matrigel matrix exhibited a spikier, less compact morphology. Cells did not recover as well after splitting.

Cells were transfected using a lipid mediated transfection method with Cas9GFP, LMNA Guide 1, and HGPS ssODN containing the GGC to GGT mutation at position 1824. Cells were imaged 24 hours after transfection. Overall, cells under the Geltrex/StemFlex conditions survived better than those under the Matrigel/mTeSR1 conditions (Figure 8, Figure S6). The presence of GFP was analyzed using the microscope and surprisingly, cells cultured in mTeSR1 showed a higher percentage of GFP positive cells.

Figure 8:

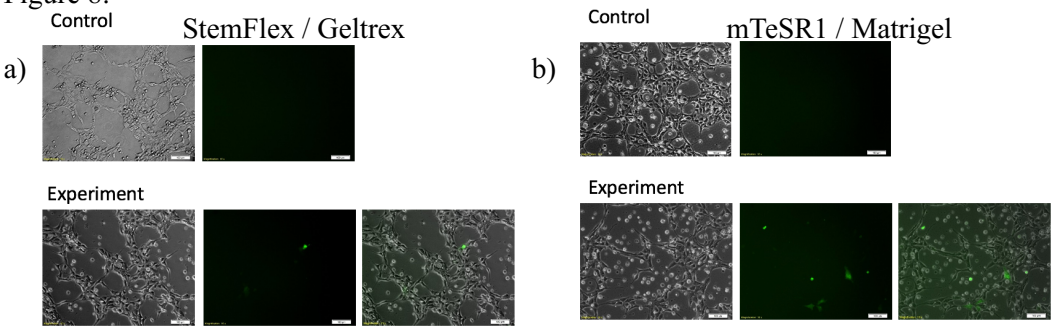

Figure 8: Survival of BJ SiPS-C after Lipofectamine 3000 transfection containing LMNA Guide 1, Cas9GFP, and ssODN containing single basepair change at site of HGPS mutation. Images captured 24 hours post transfection. a) BJ SiPS-C replated in StemFlex / Geltrex conditions exhibited better survival post transfection. b) BJ SiPS-C replated in mTeSR1 / Matrigel conditions did not recover well, although a higher percentage of GFP was observed.

Cells were dissociated and counted 48 hours after transfection, and FACS sorted based on GFP expression. FACS analysis confirmed that BJ SiPS-C cultured in Matrigel/mTeSR1 had a much higher percentage of GFP positive cells at 17.0%, while those cultured in Geltrex/StemFlex showed 3.3% GFP positivity.

Table 1:

Geltrex / StemFlex		Matrigel / mTeSR1	
Cell Counter	**Hemocytometer**	**Cell Counter**	**Hemocytometer**
Ctrl: 5.73 x 10^5 cells	Ctrl: 7.53 x 10^5 cells	Ctrl: 1.16 x 10^6 cells	Ctrl: 1.05 x 10^6 cells
Exp: 2.1 x 10^6 cells	Exp: 2.59 x 10^6 cells	Exp: 1.8 x 10^6 cells	Exp: 1.13 x 10^6 cells

Table 1: Transfected BJ SiPS-C were harvested 48 post transfection and counted using an automated cell counter and hemocytometer. Cells cultured on Geltrex / StemFlex exhibited higher cell counts than those cultured on Matrigel / mTeSR1, consistent with microscopy data.

Figure 9:

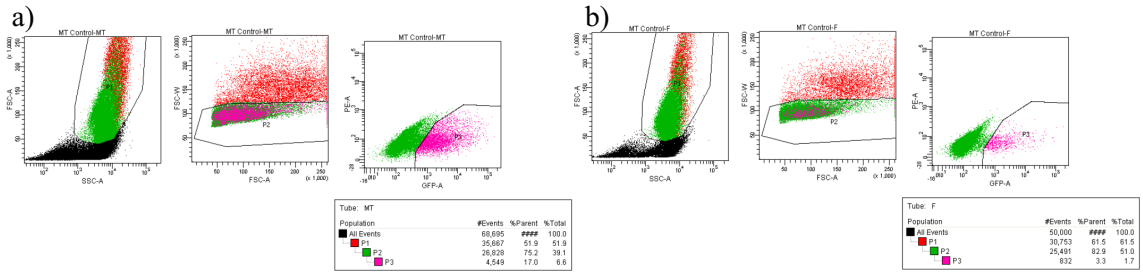

Figure 9: 48 hours post transfection, cells were harvested and sorted based on presence of GFP. To ensure a pure population and avoid false positives, GFP was gated strictly. a) BJ SiPS-C cultured on Matrigel / mTeSR1 after transfection showed a 17.0% GFP positive population, and cells cultured on Geltrex / StemFlex after transfection showed a 3.3% GFP positive population.

6.2 x 10^5 cells were collected for each condition and plated on three ten centimeter dishes. Survival post FACS was assessed by counting the number of colonies growing within a period of 7 days. Under Geltrex/StemFlex conditions, an average 1184 colonies per ten cm dish survived, while on Matrigel/mTeSR1 conditions, an average of 575 colonies. On each of the 96 well plates with 1 sorted cell/well only 3 colonies survived for each condition. Single colonies from the 10cm dishes were picked onto six 96 well plates,

three for each condition. The remaining colonies were harvested, and a TIDE analysis showed that nuclease activity was consistent from HEK293T to iPS. LMNA Guide 1 showed a slight increase in cutting efficiency in the BJ SiPS-C cells than in the HEK293T cells at 53.6% under Matrigel/mTeSR1 conditions, and 45.2% under Geltrex/StemFlex conditions (Figure S8).

gDNA was extracted from each clone of the three plates being cultured on Geltrex/StemFlex. The region of interest was PCR amplified and run on a 1% agarose gel (Figure 9, Figure S9).

Figure 10:

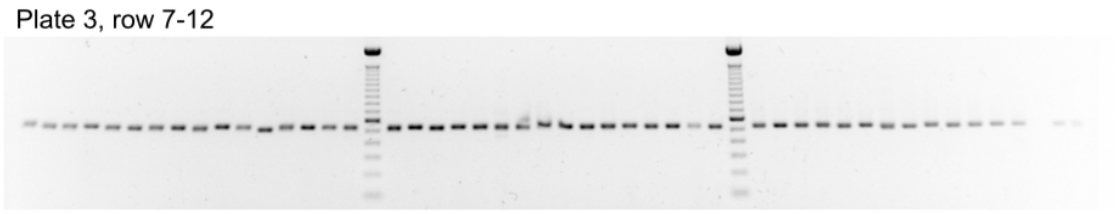

Figure 10: After single colonies were picked, gDNA was extracted and the region of interest was amplified using the conditions optimized in earlier experience. The presence of a 526 bp band indicated a successful amplification. PCR products were sent for Sanger sequencing. Image courtesy of Benjamín Erranz.

PCR products were sent for Sanger sequencing and the sequences were analyzed for editing efficiency using Geneious software.

Table 2:

	Plate 1	Plate 2	Plate 3
No cutting	1.04 %	2.08 %	11.46 %
Indels	18.75 %	21.9 %	78.13 %
Knockin	1.04 % (1 het)	0 %	2.08 % (1 het, 1 homo)
Inconclusive	79.1 %	76.0 %	8.3 %

Table 2: Genome edited clones were sent for sequencing to determine if the if the C to T mutation at position 1824 took place, and to quantify the cutting efficiency in iPSCs. 2.08% of clones exhibited a genotype indicative of a knock-in event.

Sequence analysis data was consistent with TIDE results, and in some cases showing an even higher number of cutting events in the case of plate 3, which showed a 78.13% indel rate. Out of 288 clones sequenced, 3 clones showed evidence of a knock-in event. Two out of three of these knock-ins were heterozygous, while one was homozygous.

Aim 1b

iPSC Reprogramming

HGPS patient fibroblasts from a 14 year old male were reprogrammed in conjunction with WT neonatal fibroblasts. NM-RNA reprogramming was significantly more efficient than Sendai virus reprogramming. From the Sendai virus transduced HGPS fibroblasts, only one iPS colony was picked. Using the NM-RNA reprogramming method, a total of 6 colonies were picked from transfected HGPS fibroblasts, and 12 were picked from transfected BJ fibroblasts. Morphology changes were evident starting immediately after transfection (Figure 11, S11).

Figure 11: a)

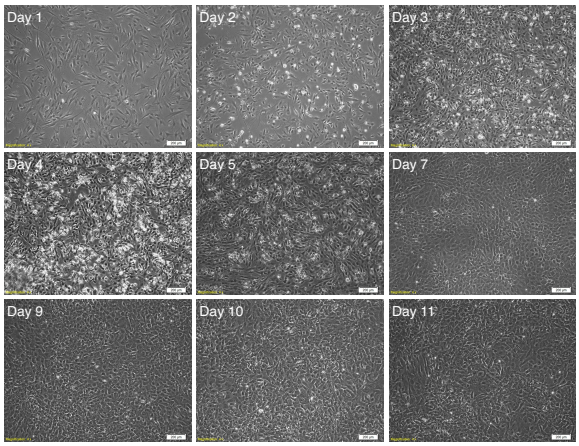

b)

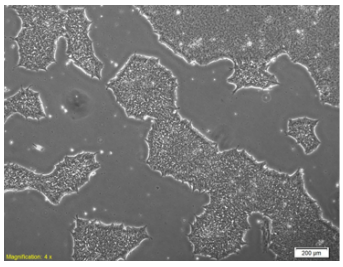

Figure 11: Morphology change during NM-RNA reprogramming progress of fibroblasts. a) Day 1 fibroblasts until Day 11 post transfection. b) HGPS iPSC-6 successfully reprogrammed from fibroblasts, picked roughly ten days post transfection. Image courtesy of Benjamín Erranz.

Fibroblasts reprogrammed using the NM-RNA method exhibited a much more ESC-like morphology than the colony picked from the Sendai reprogramming method. Two HGPS iPSC lines were sent for karyotype analysis, and pluripotency markers were tested using ICC. Nanog, Oct4, SSEA3, SSEA4, and TRA-1-60 were all expressed in reprogrammed iPSC lines (Figure 12, S10).

Figure 12:

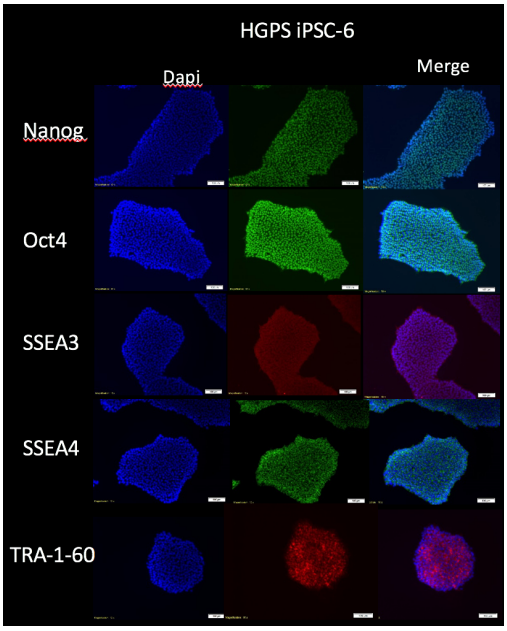

Figure 12: Reprogrammed iPSCs were tested for the presence of plurpotency markers using ICC. Cells were positive for Nanog, Oct4, SSEA3, SSEA4, and TRA-1-60 indicating cells were successfully reprogrammed back into a pluripotent state.

qRT-PCR was used to test for the presence of the pluripotency markers Lin28, Oct4, and Sox2 (Figure 13). All three genes were reactivated in both WT and diseased reprogrammed iPSCs. However, iPSCs derived from HGPS patients showed significantly less expression compared to control iPSCs for all three markers, especially Oct4 and Sox2.

Figure 13:

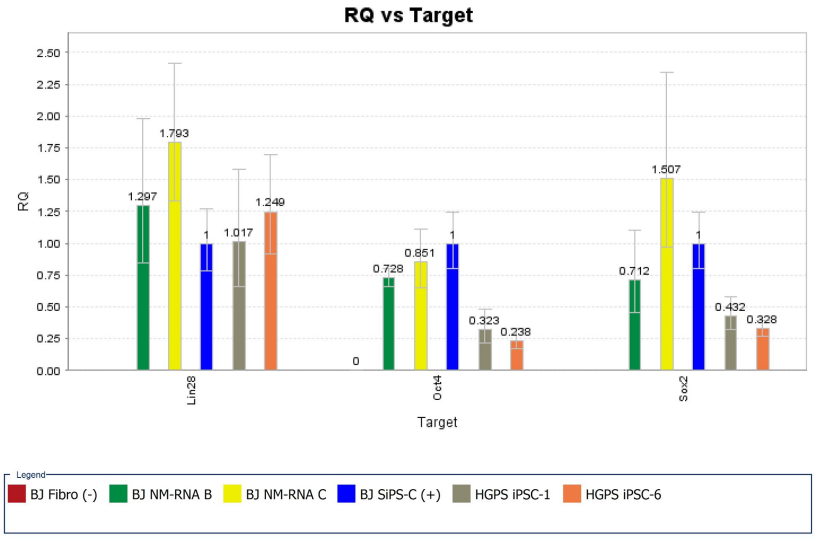

Figure 13: Reprogrammed iPSCs showed an up-regulation Lin28, Oct4, and Sox2 as compared to BJ fibroblasts and comparable levels to WT iPSCs indicating cells were successfully reprogrammed to a pluripotent state.

qRT-PCR was also used to confirm differentiation potential of all reprogrammed iPSC lines (Figure 14).

Figure 14:

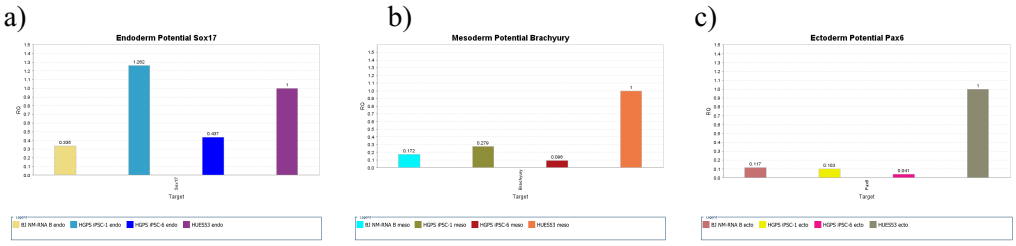

Figure 14: Reprogrammed iPSCs were differentiated directly into the three germ layers: endoderm, mesoderm, and ectoderm. Cells differentiated into all three germ layers, expressing Sox17, Brachyury, and Pax6 respectively.

Endoderm potential was measured based on Sox17 expression, mesoderm on Brachyury expression, and Ectoderm on Pax6 expression. Levels of these markers were all upregulated in cells that underwent directed differentiation towards their respective lineage. Pax6 expression was lower as compared to Sox17 and Brachyury.

Aim 2

Cardiomyocyte Differentiation

HGPS and BJ NM-RNA iPSCs were differentiated in to cardiomyocytes using a Wnt signaling inhibitor pathway. Of the differentiated iPSCs, WT BJ iPSCs exhibited a more robust beating pattern than those differentiated from HGPS iPSCs (Movie). After cells were induced towards the cardiomyocyte lineage, they began to exhibit a compact, webbed, morphology (Figure 15). Cells began to beat 9 days after induction (S12, S13, S14).

Figure 15:

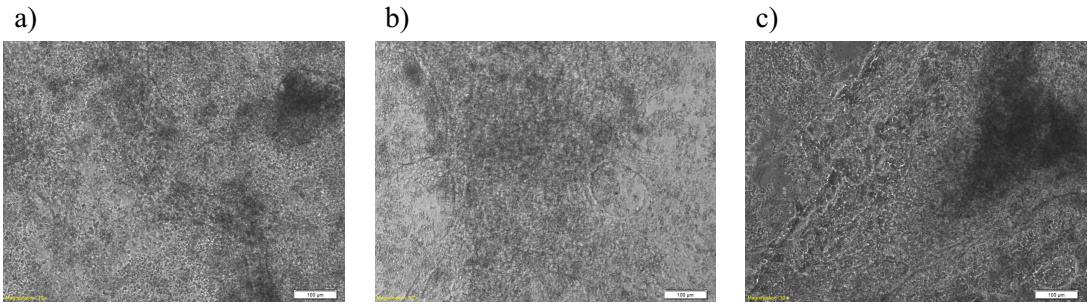

Figure 15: Cardiomyocyte morphology. Cardiomyocytes exhibit a 3D, compact, webbed morphology. a) BJ NM-RNA B cardiomyocytes b) HGPS-1 cardiomyocytes c) HGPS-6 cardiomyocytes.

ICC was used to test for TNNT (cardiac troponin) and NKX2.5, markers of cardiomyocytes. Differentiated cardiomyocytes exhibited clear expression of TNNT, but no expression of NKX2.5 was observed (Figure 16).

Figure 16:

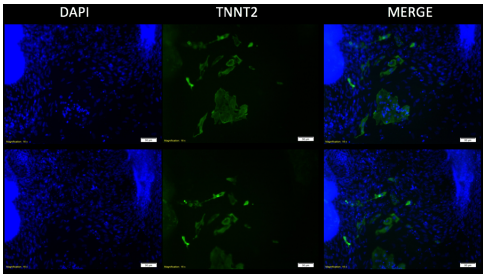

Figure 16: Cardiomyocytes derived from HGPS iPSC-6 exhibit a clear expression of TNN2- Cells were stained 21 days after induction, and 10 days after they began to beat.

To determine the cardiomyocyte population post differentiation, cells were harvested and stained with TNNT and SIRPA, a cardiomyocyte surface marker and analyzed by FACS (Figure 17).

Figure 17:

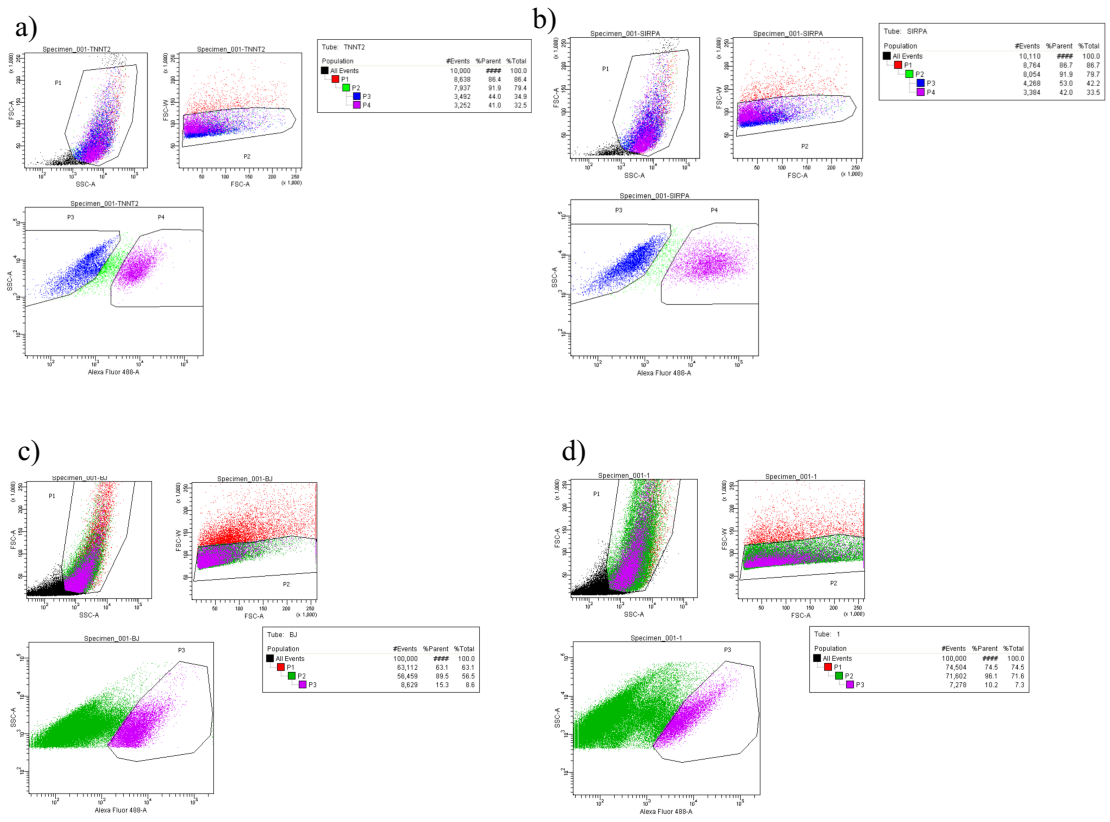

Figure 17: a-b) Cardiomyocytes differentiated from BJ NM-RNA iPSC B were analyzed through FACS for the presence of the cardiac markers SIRPA and TNNT2 21 days after starting the differentiation and 11 days after they began to beat. Roughly 40% of the differentiated cell population expressed these markers indicating a successful differentiation. c) Roughly 15% of cell population from cardiomyocytes differentiated from BJ NM-RNA iPSC B expressed SIRPA 15 days after starting differentiation. d) Roughly 10% of cells population from cardiomyocytes differentiated from HGPS iPSC-1 expressed SIRPA 15 days after starting differentiation.

41.0% of the differentiated population expressed TNNT2, while 42.0% expressed SIRPA at Day 21. Although the differentiation protocol did yield a population of around 40.0% cardiomyocytes, it is still not a pure population. In another trial, 15% of the cell population differentiated from BJ NM-RNA iPSC B expressed SIRPA, and 10% of the cell population differentiated from HGPS iSPC-1 expressed it at Day 15. These cells were sorted for further analysis (Figure 17).

To further characterize the population of differentiated cardiomyocytes, qRT-PCR was used to measure levels of the cardiac markers ACTC1, BNP, MYH7, NKX2.5, and TNNT2 (Figure 18).

Figure 18:

a)

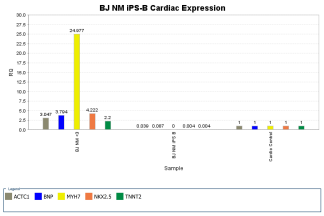

b)

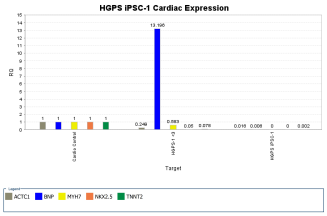

c)

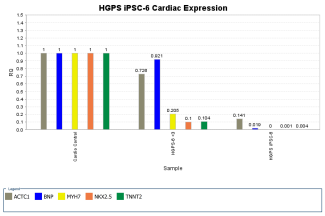

d)

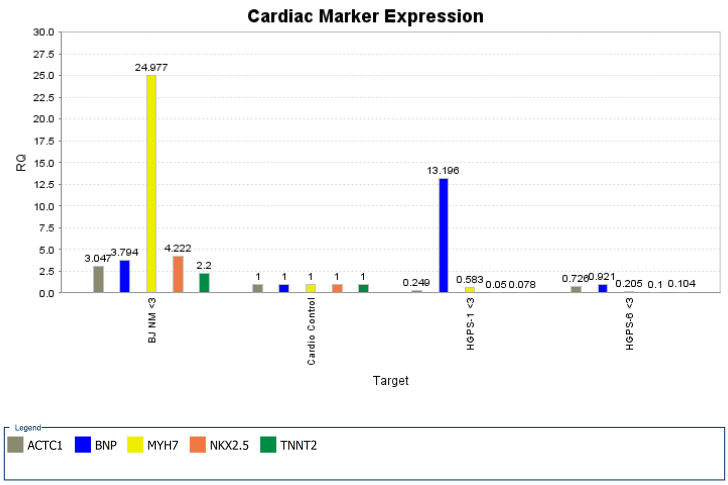

Figure 18: Markers of cardiac expression. a) Cardiomyocytes derived from BJ NM-RNA expressed upregulated levels of cardiac markers as compared to their undifferentiated state. b) Cardiomyocytes derived from HGPS iPSC-1 showed a small upregulation of cardiac markers as compared to their undifferentiated state, and a spike in BNP levels was observed. c) Cardiomyocytes derived from HGPS iPSC-6 expressed upregulated levels of cardiac markers as compared to their undifferentiated state. d) A comparison of BJ NM-RNA cardiomyocytes and cardiomyocytes derived from HGPS iPSCs.

Cardiomyocytes differentiated from iPSCs derived from both BJ fibroblasts and HGPS fibroblasts exhibited an up regulation of all observed cardiac markers as compared to their undifferentiated state. Consistent with differences in beating patterns, cardiomyocytes differentiated from BJ NM-RNA iPSC-B showed higher expression of cardiac markers as compared to those differentiated from HGPS iPSCs.

Aim 3

Changes in Gene Expression in HGPS Patients

After reprogrammed iPSCs were differentiated to cardiomyocytes, levels of cardiac markers were measured (Figure 19). With the exception of BNP, levels of all cardiac markers were lower in diseased HGPS iPSCs as compared to WT BJ iPSCs.

Figure 19:

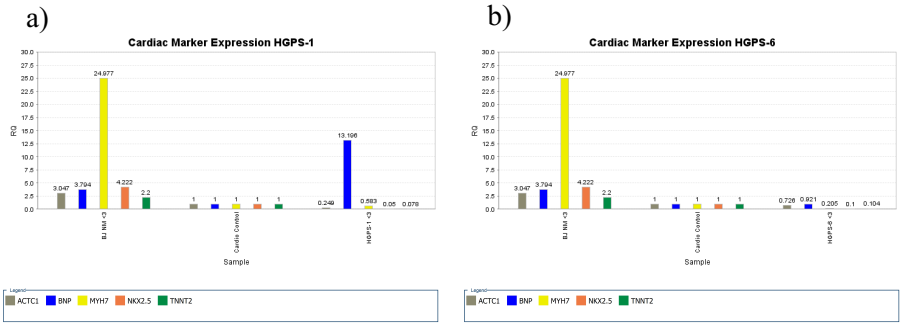

Figure 19: Changes in cardiac differentiation potential in HGPS patients. With the exception of BNP, levels of cardiac markers were decreased in cardiomyocytes derived from iPSCs reprogrammed from HGPS fibroblasts as compared to cardiomyocytes differentiated from WT iPSCs.

Cell populations resulting from cardiomyocyte differentiation of WT and HGPS iPSCs were purified using the surface cardiac marker, SIRPA. Levels of cardiac markers of this pure population were analyzed using qRT-PCR and compared to levels in undifferentiated and mixed cell populations (Figure 20).

Figure 20:

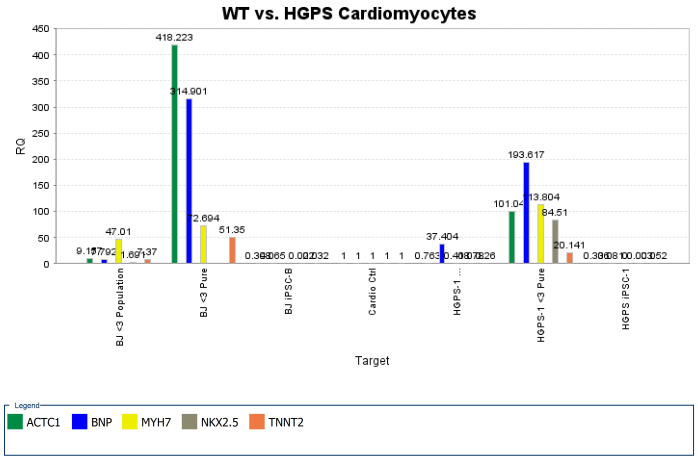

Figure 20: WT and HGPS cardiomyocytes isolated based on SIRPA expression compared to undifferentiated and mixed cell type population

Pure cardiomyocyte populations exhibit a greater expression level of all cardiac markers as compared to their undifferentiated and mixed population counterparts.

HGPS iPSCs and WT BJ iPSCs underwent tri-lineage directed differentiation. RNA was extracted and reverse transcribed to cDNA. RT-PCR was performed to determine the presence of the truncated form of LMNA associated with HGPS (Figure 21).

Figure 21

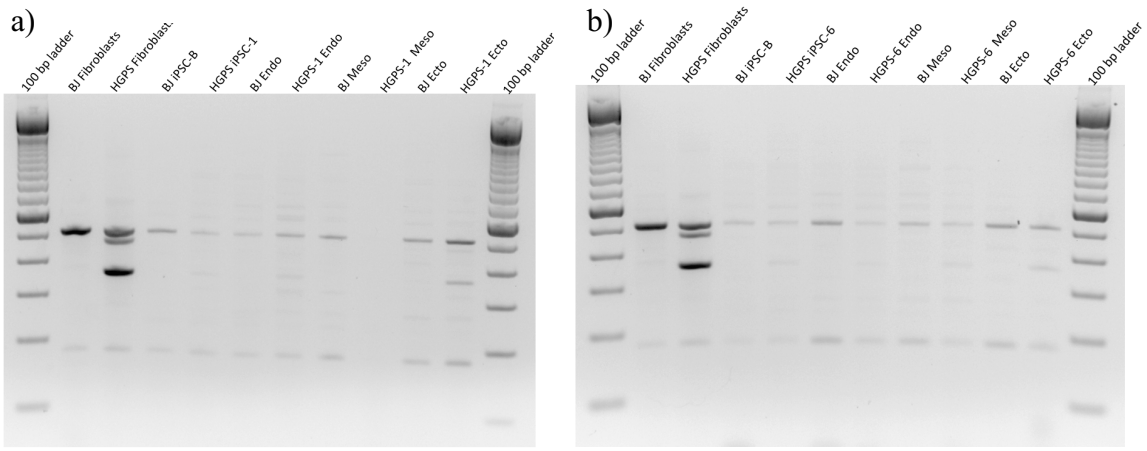

Figure 21: The presence of truncated form of LMNA. a) HGPS iPSC-1 b) HGPS iPSC-6. The presence of the truncated form of LMNA that occurs as a result of alternative splicing is evident by two bands, the in tact transcript at 510 bp, and the mutant transcript at 360 bp. Levels of mutant transcript disappear in iPSCs, and are evident at varying levels in different lineage populations.

WT BJ fibroblasts showed one band indicating that LMNA is intact, while HGPS fibroblasts exhibited two bands indicating that alternative splicing has taken place. After being reprogrammed to iPSCs, the presence of the second band diminished, but was present in HGPS endoderm, mesoderm, and ectoderm lineage populations in different amounts.

This RT-PCR was repeated on cardiomyocytes derived from WT and HGPS iPSCs. Purified populations of the resulting cardiomyocyte populations were also included to see whether or not there was a difference in levels of truncated LMNA (Figure 22).

Figure 22:

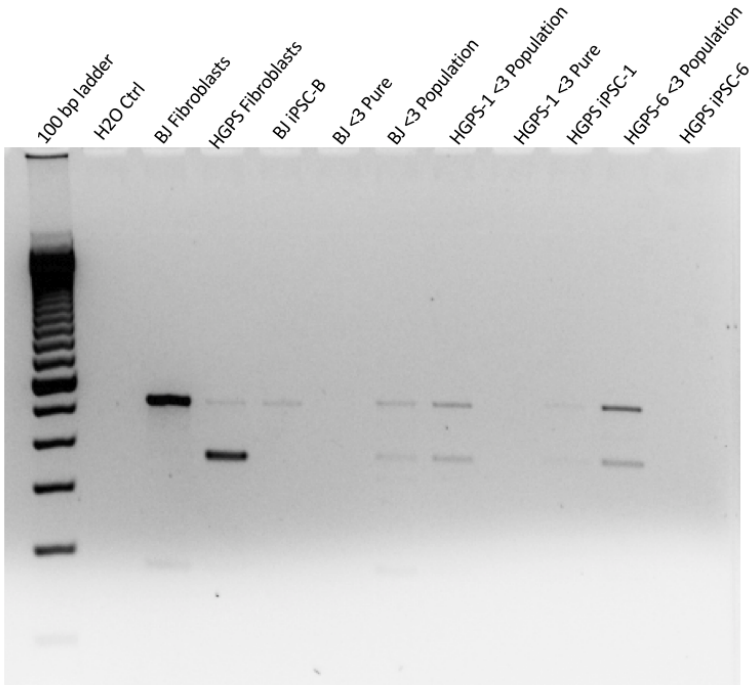

Figure 22: The presence of truncated form of LMNA in cardiomyocytes derived from WT and HGPS fibroblasts. The presence of the truncated form of LMNA that occurs as a result of alternative splicing is evident by two bands, the in tact transcript at 510 bp, and the mutant transcript at 360 bp. Levels of mutant transcript disappear in iPSCs, and are evident at varying levels in different cardiomyocyte populations.

Pure population cardiomyocytes did not yield product. The presence of two bands is weak or nonexistent in iPSC populations, and evident to varying degrees in cardiomyocyte full population samples.

Chapter IV. Discussion

Hutchinson-Gilford Progeria Syndrome is an extremely rare premature aging disease that unfortunately has no cure. There is still much to be learned about the pathology of this disease and what aspects of it can be targeted for treatments. The purpose of this research was to create a platform in the form of model cardiomyocytes for studying the effects of the silent glycine mutation at position 1824 in the LMNA gene that causes HGPS, and to begin to understand how the mutation affects this specific cell type.

Conclusions

Genome Editing | BJ SiPS-C was targeted using the CRISPR Cas9 system to introduce the mutation responsible for HGPS in the LMNA gene. Although the first round of targeting yielded knock-in clones, the locus that was targeted was incorrect, so a second round was initiated. Guide RNAs generated in the second round of genome editing experiments did not exhibit adequate nuclease activity (Figure S5). There are multiple reasons why this could be. There could be a number of off target cutting events taking place, and it is possible that this area of the LMNA gene is not accessible for the Cas9 nuclease to bind to. Concurrently, it was determined that culturing iPSCs on Geltrex / StemFlex medium allowed the cells to exhibit a healthier morphology and increase survival after FACS sorting (Figure 7).

Reprogramming | As an alternative to obtaining HGPS iPSCs from genome editing experiments, BJ fibroblasts and fibroblasts from an HGPS patient were reprogrammed to iPSCs using the Sendai virus and NM-RNA reprogramming methods. Both cell types yielded iPSCs, however an increased number of iPSCs were generated from the BJ fibroblasts as compared to HGPS fibroblasts. Additionally, the Sendai method only yielded one iPS clone from HGPS fibroblasts. The low efficiency in reprogramming could be due to the health of the diseased starting material. Low efficiency of HGPS fibroblast reprogramming was previously reported. The newly derived iPS lines were tested to confirm their pluripotent state. Although HGPS and BJ iPS lines reactivated the expression of Oct4, Sox2 and lin28, the HGPS lines displayed a lower expression of these markers compared to BJ derived iPS lines. LMNA is known to be expressed in somatic cells but absent in embryonic stem cells. However, by RT-PCR, residual expression of LMNA was observed in the HGPS iPS lines (Figures 21,22).

Cardiomyocyte Differentiation | iPSCs reprogrammed from WT BJ fibroblasts and HGPS fibroblasts were differentiated in to cardiomyocyte. There was a clear difference in beating patterns, morphology, and levels of cardiac markers in cardiomyocytes differentiated from BJ iPSCs compared to HGPS iPSCs. WT cardiomyocytes exhibited a much more cohesive, quick, beating pattern, and also overall expressed cardiac markers at a higher level than HGPS cardiomyocytes (S12-S14). It is to be expected that the disruption of the nuclear membrane caused by the HGPS mutation makes it more difficult for certain cell types to develop properly. Cardiomyocytes selected for and sorted based

on the presence SIRPA exhibited a higher level of cardiac markers than their mixed population counterparts (Figure 20). This clear difference solidifies the need to ensure that the population of cardiomyocytes (or any cell type) needs to be as pure as possible for data obtained to be conclusive.

Changes in gene expression levels in HGPS | Success in aims one and two allowed changes in gene expression levels in HGPS to be explored. Levels of cardiac markers were observed to be lower in HGPS cardiomyocytes as compared to WT using both FACS and qRT-PCR (Figure 17, 18). This suggests an interference in the cardiomyocyte differentiation process caused by the HGPS mutation. Hypertension is a major symptom of the disease, therefore we looked at the expression of BNP in HGPS versus BJ cardiomyocytes. BNP (B-type Natriuretic peptide) is a hormone produced by the heart that was shown to be elevated in patients with hypertension. The level of BNP expression was not consistent between the two iPS lines derived from the HGPS patient and was also very different between the unsorted and sorted population. These experiments should be repeated to understand the source of this disparity.

The interference of the HGPS mutation is also evident when visualizing the presence of the mutant form of LMNA on a gel after RT-PCR in the three germ layers. There is a clear shift from a strong presence of progerin in fibroblasts to a residual expression in iPSCs derived from those same fibroblasts. The presence of the spliced mutant form appears again in populations that were differentiated directly in to the three germ layers, and in cardiomyocytes derived from these iPSCs (Figure 21). It was

previously shown that the level of expression of the spliced mutant form is correlated to the severity of the disease. Interestingly, ectoderm lineages exhibited the strongest signal of the truncated form of LMNA. While skin development is greatly affected in HGPS patients, neuronal cells remain healthy. After cardiomyocytes differentiation, the level of the truncated form of LMNA was significantly increased, confirming an important contribution of this cell type in the disease.

Study Limitations

Although this study was successful in creating a platform in which to study HGPS in cardiomyocytes, this study was not without its limitations. The biggest limitation is working with an impure cardiomyocyte population. Until protocols are optimized to maximize the number of cardiomyocytes obtained at the end of the differentiation process, or protocols to enhance purity are improved, it is difficult to make conclusions regarding expression levels of certain genes, as it is uncertain whether the levels are due to changes in cardiomyocytes or from other cell types. We sorted the cardiomyocytes using an antibody against SIRPA, a surface marker specific of cardiomyocytes, but the number of sorted cells was low, limiting the data obtained from them. Increased number of trials must be executed to solidify any speculations and hypotheses formed based on preliminary data.

Lastly, it was difficult to observe nuclear blebbing in HGPS fibroblasts and cells differentiated from HGPS iPSCs. This difficulty is most likely due to complications of

the Lamin A/C and Progerin antibodies to aid in visualizing the mutant phenotype, such as using an inadequate concentration of antibody.

Future Research Directions

The derivation of HGPS iPS lines and their differentiation into cardiomyocytes allowed us to obtain preliminary data on the roles of these cells in the disease.. Further experiments to quantify levels of the mutant form of LMNA, progerin, can be performed in differentiated cell populations to determine its effect on their development. Western blot analysis could confirm the level of Progerin expression detected by q-RT-PCR . Furthermore, qRT-PCR experiments may be performed and melting curves of the two products (WT LMNA and progerin) can be discriminated for and quantified. This will also provide insight as to how much of this protein is actually present in different differentiated cell populations, and if there is a difference in development of the three germ layers.

The ability to differentiated HGPS iPSCs in to cardiomyocytes has opened the door for further disease modeling and drug testing. Improvements to cardiomyocyte differentiation protocols and enhancing the purity of these differentiated populations will give an even better model to work with. It will also be interesting to differentiate the obtained HGPS iPSCs in to other cells types such as hepatocyte like cells, as hepatocytes are another major cell type affected in HGPS patients (Ulrich *et al.* 2015).

Further experimentation can be performed on the derived HGPS cardiomyocytes to look at levels of other cardiac markers indicative of hypertension, like angiotensin

converting enzyme (ACE), and to look at levels of DNA methylation to see if they are comparable to those of an aged person (Oudit *et* al. 2003, Liu *et al.* 2011).

Lastly, to eliminate the use of patient fibroblasts all together, genome editing of the LMNA gene will be revisited. Because HGPS is such a rare disease, not having to rely on a patient sample is critical to maximize the amount of disease modeling performed. Another major advantage in using genome editing to create HGPS model is the possibility to derive isogenic lines, offering a better control than the BJ iPS lines used in our study.

Implications & Significance of Results

The derivation of cardiomyocytes from HGPS patients with the G608G mutant through iPSCs differentiation had never been completed before, and being able to do so is significant because it provides a framework for furthering our knowledge about the pathology of the disease and disease modeling. *In vitro* experiments make studying rare diseases like HGPS easier. Preliminary findings give exciting hope for new connections to be made between levels of certain genes and diseased cardiomyocytes, and starts the process of thinking about how these cardiac cells of HGPS patients can be manipulated to mitigate the effects of the disease.

Appendix & Supplementary Figures

Figure S1:

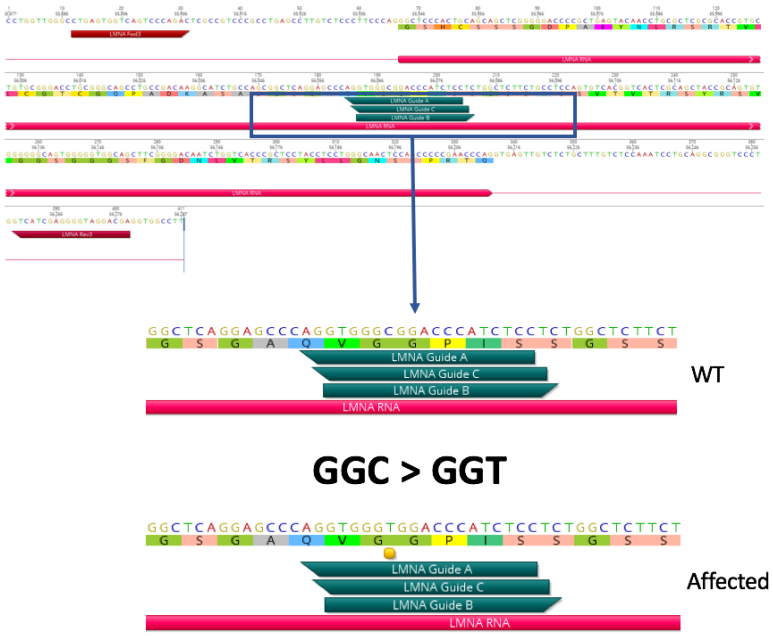

Figure 20: LMNA gene HGPS disease locus. Silent GGC > GGT mutation at position 1824 causes HGPS to develop.

Table 3:

Guide RNA	Sense Strand (5'→ 3')	Antisense Strand (5'→ 3')	Off Target Score
LMNA Guide 1	CACCGAGTTGATGAGAGCCGTACGC	AAACGCGTACGGCTCTCATCAACTC	98
LMNA Guide 2	CACCGCTGCGGGAACGGCCTGCGTA	AAACTACGCAGGCCGTTCCCGCAGC	60
LMNA Guide 3	CACCGAACACCTGGGGCTGCGGGAA	AAACTTCCCGCAGCCCCAGGTGTTC	60
LMNA Guide A	CACCG GGAGATGGGTCCGCCCACCT	AAAC AGGTGGGCGGACCCATCTCC C	80
LMNA Guide B	CACCG GTGGGCGGACCCATCTCCTC	AAAC GAGGAGATGGGTCCGCCCAC	77
LMNA Guide C	CACCG AGGAGATGGGTCCGCCCACC	AAAC GGTGGGCGGACCCATCTCCT	81

Table 3: LMNA GuideRNA sequences generated using the MIT CRISPR design tool and CRISPOR. High off target scores indicate that the guide is specific in guiding nuclease activity.

Table 4:

Primer	Fwd (5'→ 3')	Rev (5'→ 3')
LMNA	AACACCTGGGGCTGCGGGAA	CTTCGGGGACAATCTGGTCA
Actin	GGACTTCGAGCAAGAGATGG	AGCACTGTGTTGGCGTACAG
Sox17	CTCTGCCTCCTCCACGAA	CAGAATCCAGACCTGCACAA
Brachyury	AATTGGTCCAGCCTTGGAAT	CGTTGCTCACAGACCACA
Pax6	TCTAATCGAAGGGCCAAATG	TGTGAGGGCTGTGTCTGTTC
MYH17	CTGTCCAAGTTCCGCAAGGT	ATTCAAGCCCTTCGTGCCAA
ACTC1	CAGACCAGGACTTGCAACCT	TGCTCAGGGTGTCAAAGCA
NKX2.5	AGCCGAAAAAGAAAGGGTGTGA	AAAGTCAGGCTGGCTCAAGG
TNNT2	AAGAGGCAGACTGAGCGGGAAA	AGATGCTCTGCCACAGCTCCTT
BNP	TCAGCCTCGGACTTGGAAAC	CTTCCAGACACCTGTGGGAC
Lin28	Hs00702808_1	
Oct4		
Sox2	Hs01053049_s1	
RPLPO	Hs99999902_m1	
LMNA Mut	GTGGAAGGCACAGAACACCT	GTGAGGAGGACGCAGGAA

Table 4: List of forward and reverse primers used throughout the study along with melting temperature for each pair.

Figure S2:

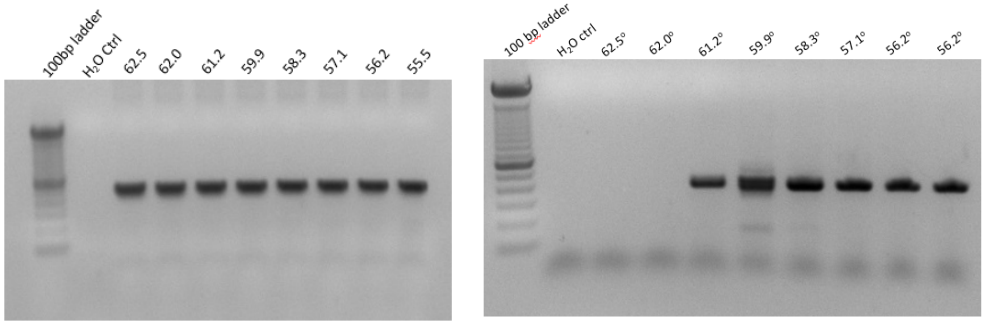

Figure S2: Temperature gradient experiments to determine optimal temperature for each primer pair. PCR reactions were carried out at an annealing temperature of 56.0 °C.

Figure S3:

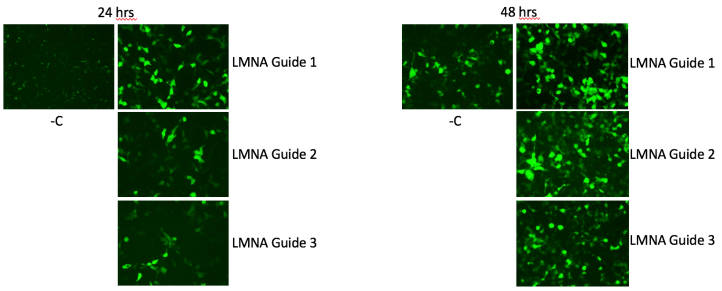

Figure S3: HEK293T cells were transfected with each RNA guide and the Cas9GFP plasmid. Presence of GFP indicates that the transfection was successful. Transfection efficiency was not altered and remained high with the addition of guide RNAs. Round 1 Lipofectamine 2000 Guide Testing.

Figure S4:

a)

b)

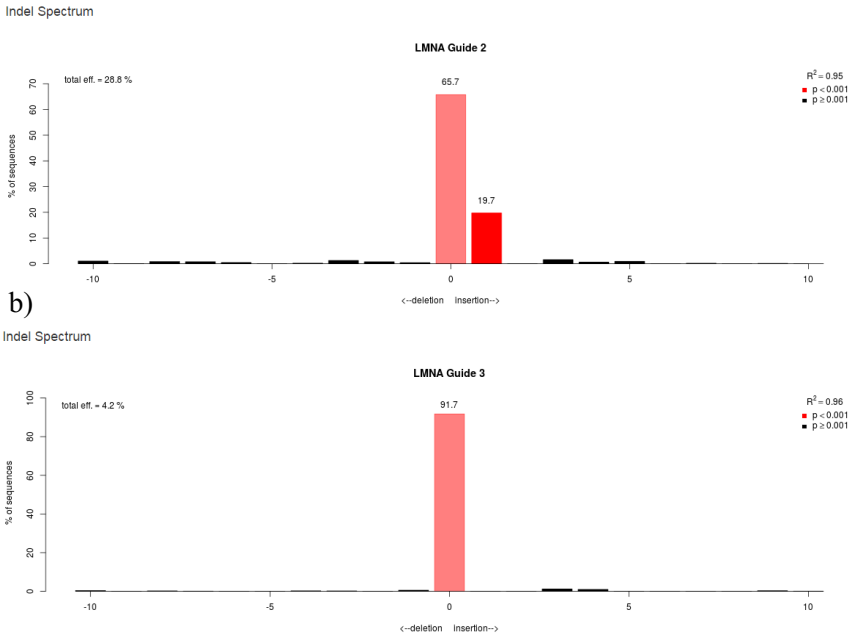

Figure S4: Sanger sequences of the uncut region of interest and the cut area of interest were compared. The tide online tool assesses mismatch in basepair peaks and area under the curve to quantify cutting efficiency in terms of insertions and deletions. a) LMNA Guide 2 performed at a 28.8% cutting efficiency, eliciting both insertion and deletion events around the cutting site of Guide 2. b) LMNA Guide 3 performed at a 4.2% cutting efficiency eliciting mainly small insertion events around the cutting site of Guide 3.

Figure S5:

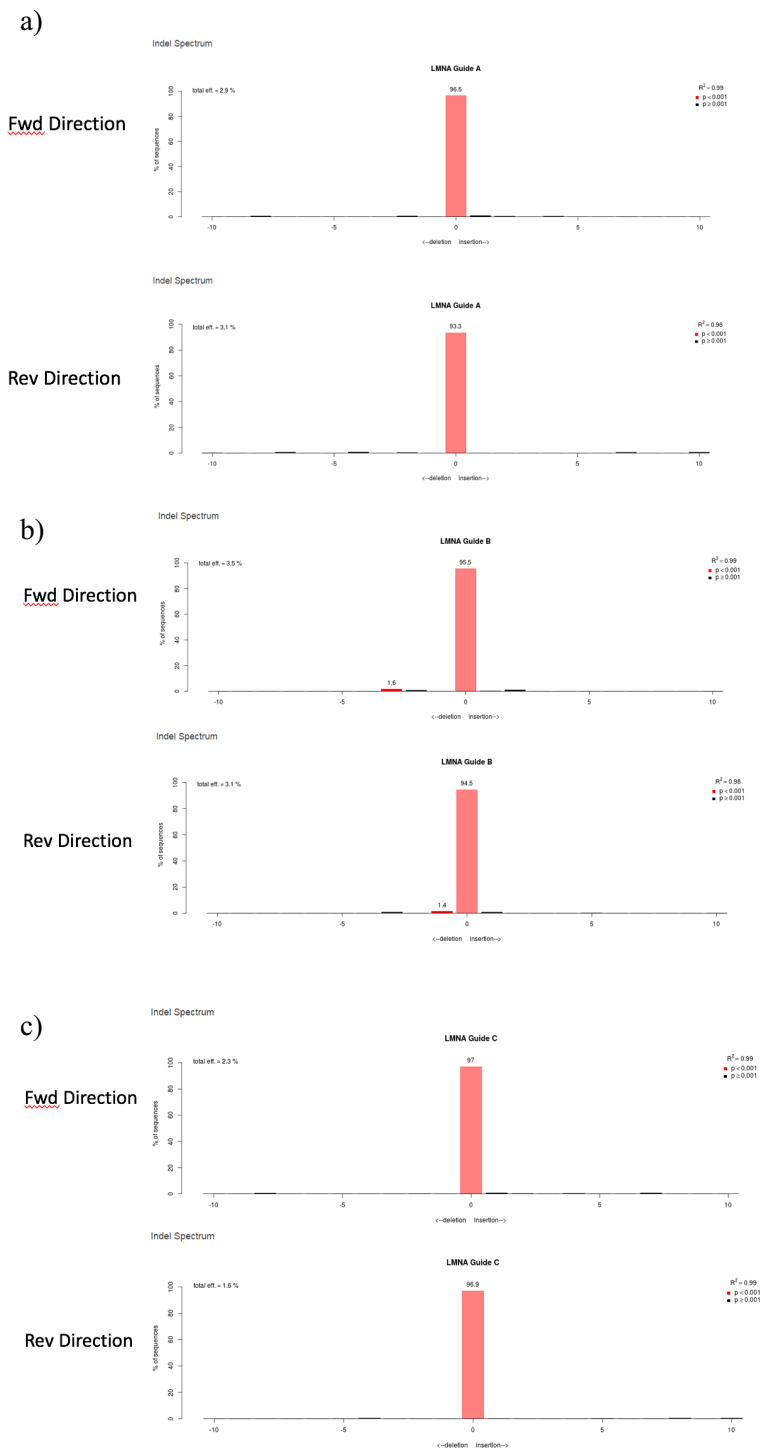

Figure S5: Sanger sequences of the uncut region of interest and the cut area of interest were compared. The tide online tool assesses mismatch in basepair peaks and area under the curve to quantify cutting efficiency in terms of insertions and deletions. a) LMNA Guide A performed at a 3.0% cutting efficiency. b) LMNA Guide B performed at a 3.3% cutting efficiency. c) LMNA Guide C performed at a 1.95% cutting efficiency.

Figure S6:

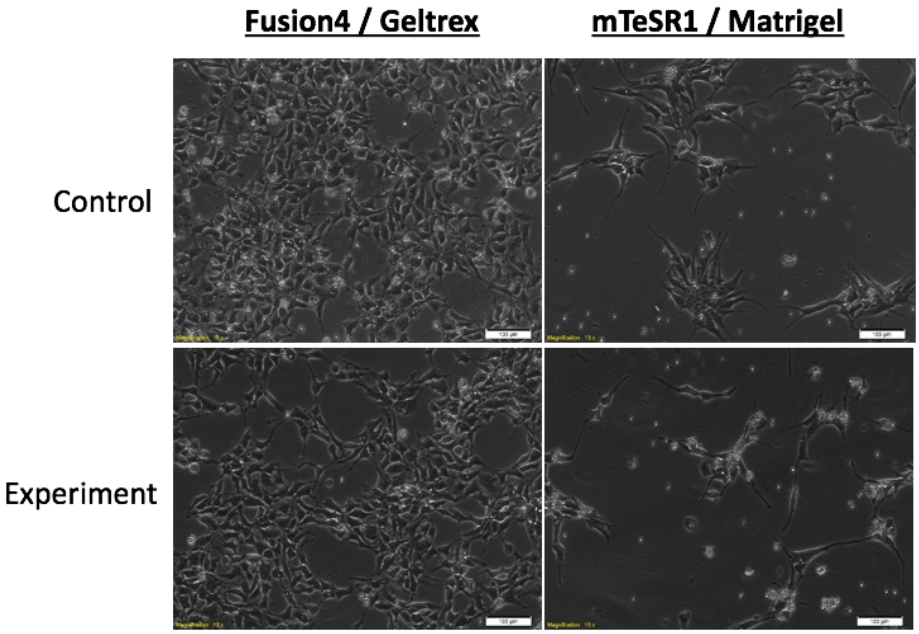

Figure S6: Survival of BJ SiPS-C after Lipofectamine 3000 transfection containing LMNA Guide 1, Cas9GFP, and ssODN containing single basepair change at site of HGPS mutation. Images captured 24 hours post transfection. a) BJ SiPS-C replated in StemFlex / Geltrex conditions exhibited better survival post transfection. No GFP observed. b) BJ SiPS-C replated in mTeSR1 / Matrigel conditions did not recover well. No GFP observed.

Table 5:

Geltrex / StemFlex	Matrigel / mTeSR1
Cell Counter	**Cell Counter**
Ctrl: 2.56 x 10^5 cells	Ctrl: 2.51 x 10^4 cells
Exp: 1.76 x 10^6 cells	Exp: 1.00 x 10^5 cells

Table 5: Transfected BJ SiPS-C were harvested 48 post transfection and counted using an automated cell counter and hemocytometer. Cells cultured on Geltrex / StemFlex exhibited higher cell counts than those cultured on Matrigel / mTeSR1, consistent with microscopy data.

Figure S7:

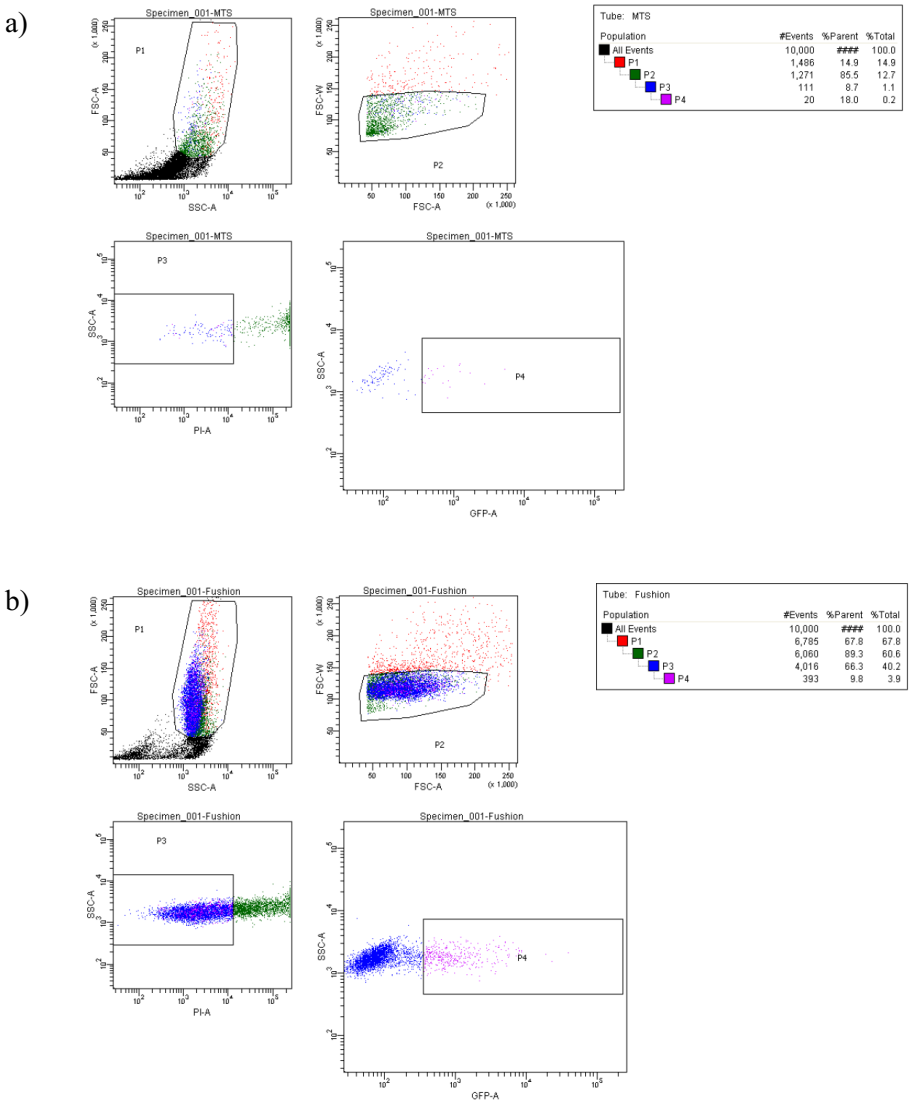

Figure S7: 48 hours post transfection, cells were harvested and sorted based on presence of GFP. To ensure a pure population and avoid false positives, GFP was gated strictly. a) BJ SiPS-C cultured on Matrigel / mTeSR1 after transfection showed a 18.0% GFP positive population b) Cells cultured on Geltrex / StemFlex after transfection showed a 9.8% GFP positive population. Results consistent with first experiment.

Figure S8:

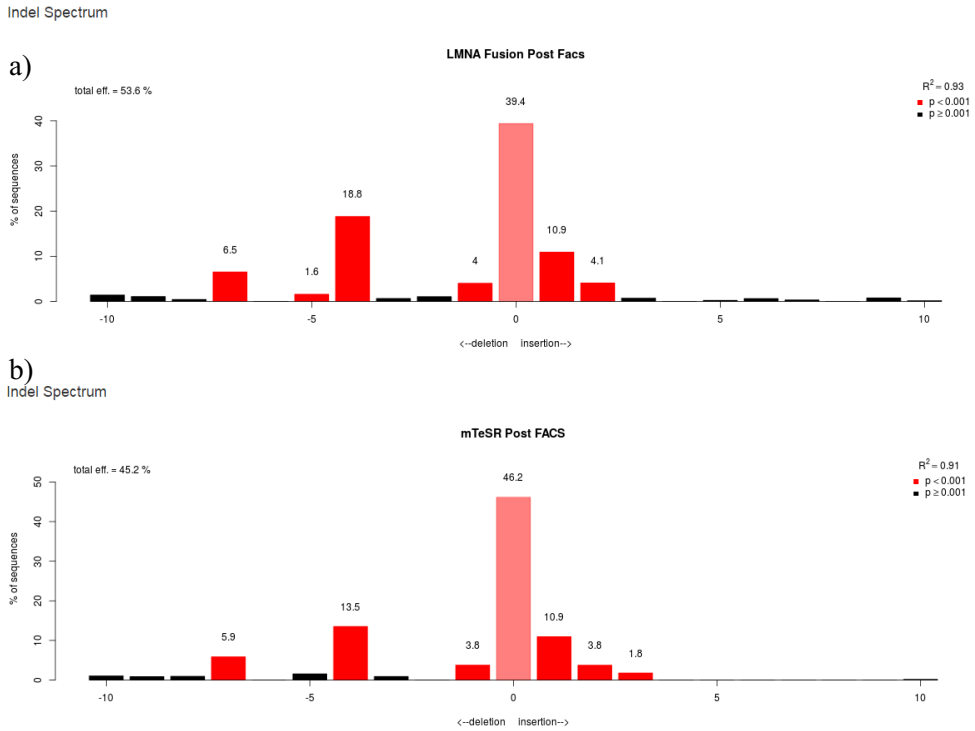

Figure S8: Sanger sequences of the uncut region of interest and the cut area of interest were compared. The tide online tool assesses mismatch in basepair peaks and area under the curve to quantify cutting efficiency in terms of insertions and deletions. a) Post FACS cell population containing cells cultured in Geltrex / StemFlex exhibited a 53.6% cutting efficiency. b) Post FACS cells population containing cells cultured in Matrigel / mTeSR1 exhibited a 45.2% cutting efficiency.

Figure S9:

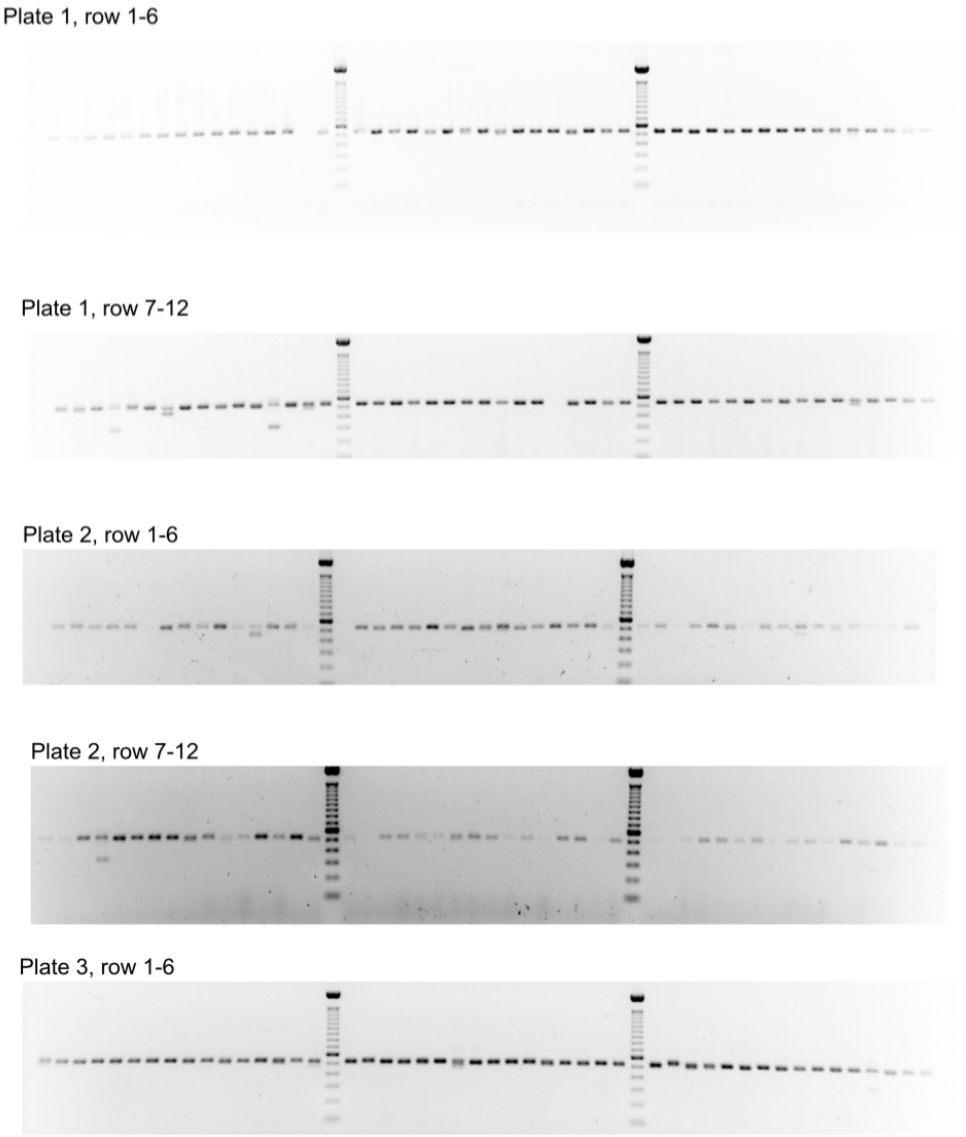

Figure S9: After single colonies were picked, gDNA was extracted and the region of interest was amplified using the conditions optimized in earlier experience. The presence of a 526 bp band indicated a successful amplification. PCR products were sent for Sanger sequencing. Image courtesy of Benjamín Erranz.

S11:

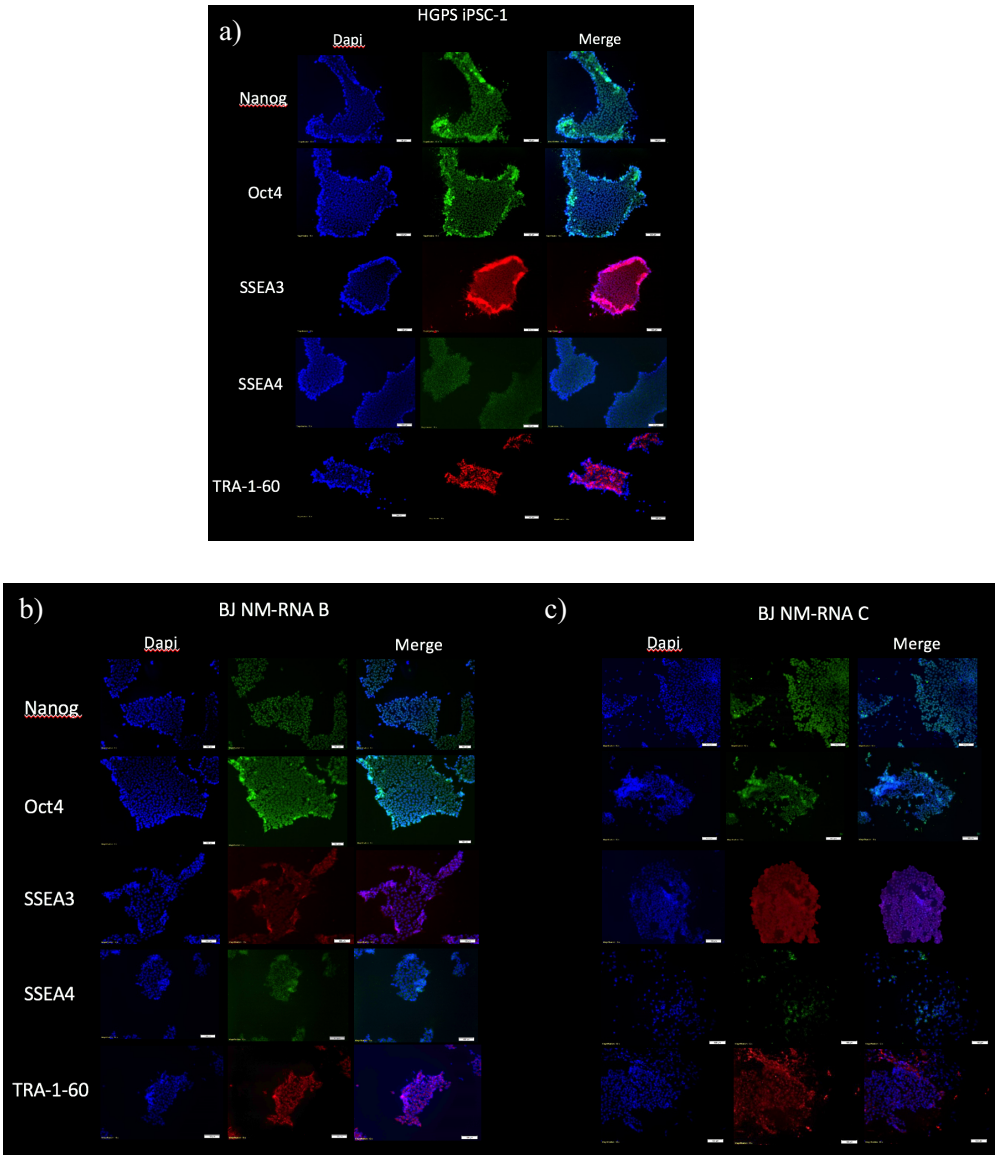

Figure S10: Reprogrammed iPSCs were tested for the presence of plurpotency markers using ICC. Cells were positive for Nanog, Oct4, SSEA3, SSEA4, and TRA-1-60 indicating cells were successfully reprogrammed back into a pluripotent state. a) HGPS iPSC-1 b) BJ NM-RNA B c) BJ NM-RNA C

S11:

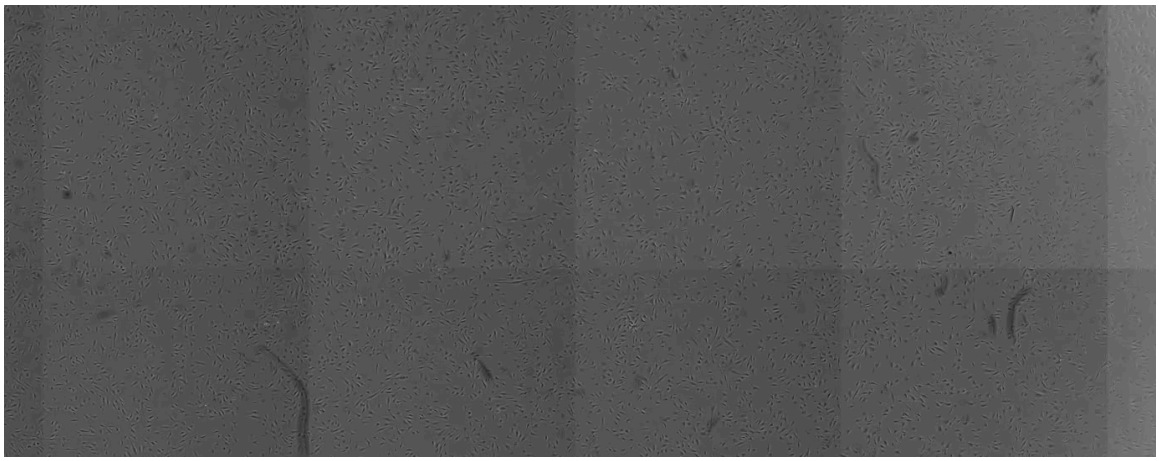

S11: BJ Fibroblasts NM-RNA reprogramming. Video courtesy of Benjamín Erranz.

S12:

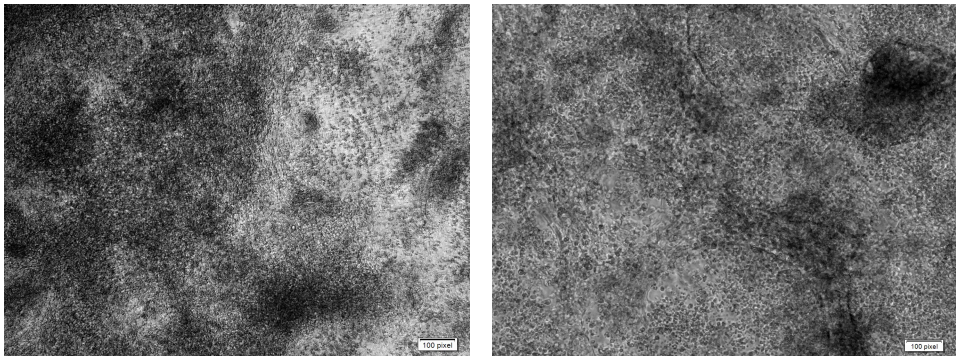

S12: Cardiomyocytes derived from BJ NM-RNA iPS B. Beating recorded 21 days after induction towards cardiomyocyte lineage.

S13:

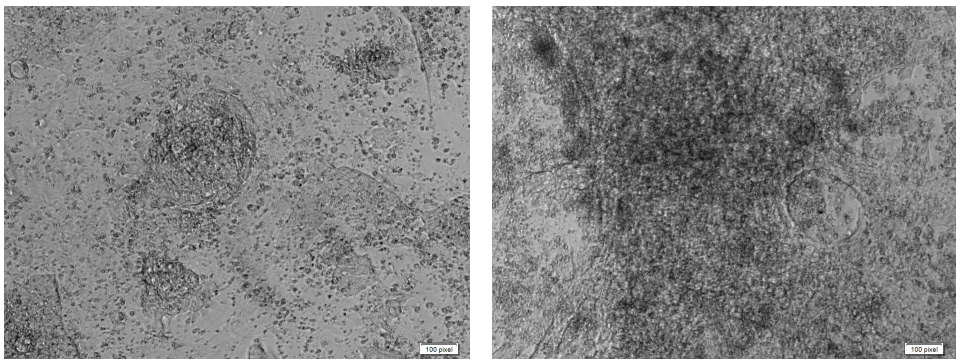

S13: Cardiomyocytes derived from HGPS iPSC-1. Beating recorded 21 days after induction towards cardiomyocyte lineage.

S14:

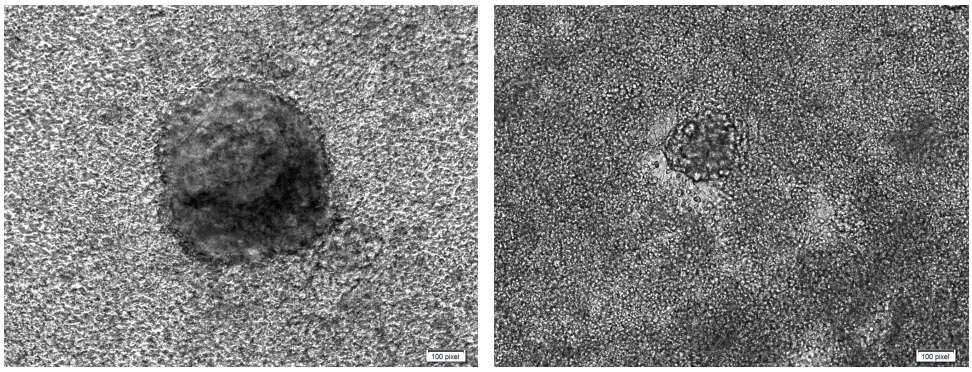

S14: Cardiomyocytes derived from HGPS iPSC-6. Beating recorded 9 days after induction towards cardiomyocyte lineage.

S15:

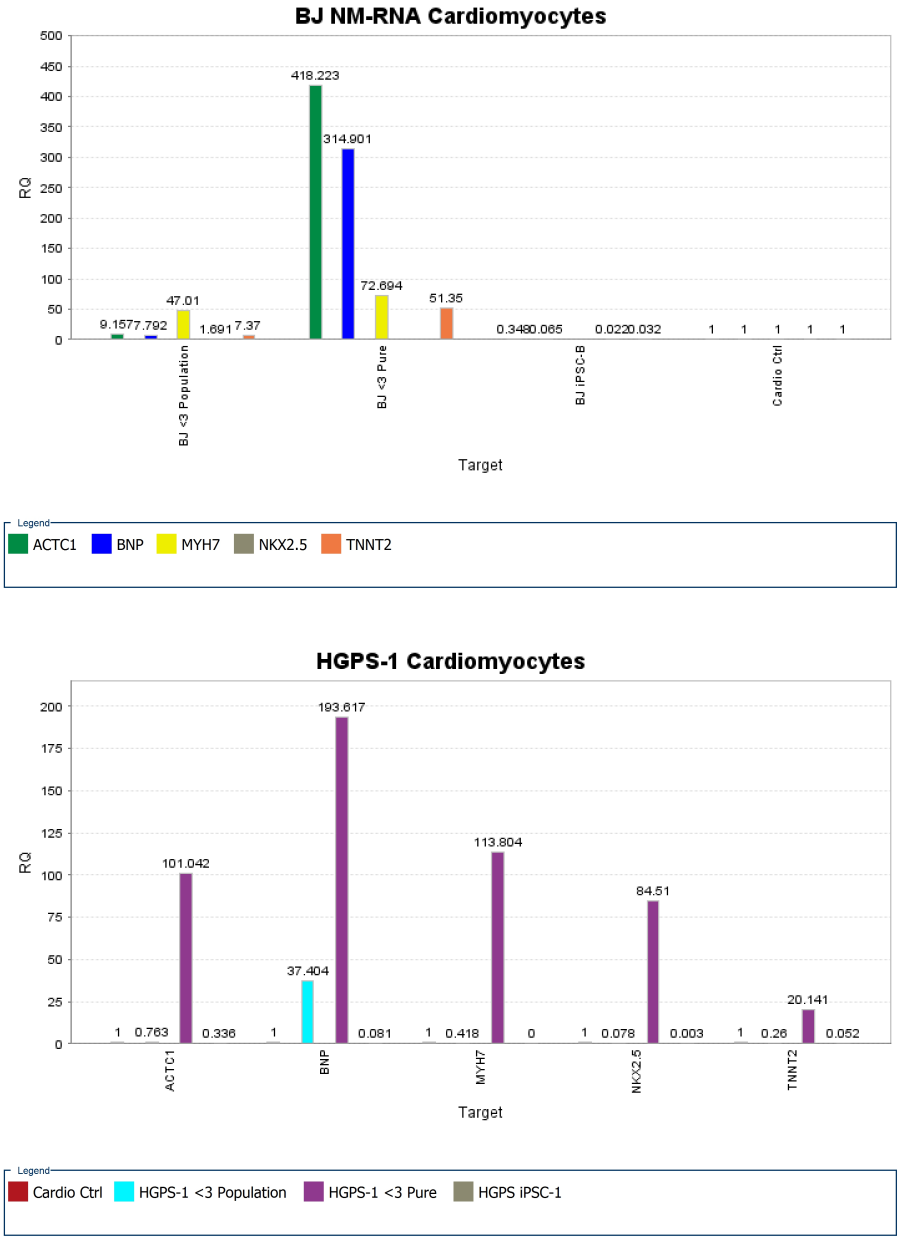

S15: Purified cardiomyocyte populations showed a higher expression level of cardiac markers than mixed populations and their undifferentiated counterparts.

References

1-s2.0-S009286740900333X-main.pdf. (n.d.). Retrieved from http://ac.els-cdn.com/S009286740900333X/1-s2.0-S009286740900333X-main.pdf?_tid=5e519008-fbd3-11e6-a38d-00000aacb360&acdnat=1488079772_41c852043dbcaebbfcb29632966fa576

Batalov, I., & Feinberg, A. W. (2015a). Differentiation of Cardiomyocytes from Human Pluripotent Stem Cells Using Monolayer Culture. Biomarker Insights, 10(Suppl 1), 71–76. https://doi.org/10.4137/BMI.S20050

Bhattacharya, S., Burridge, P. W., Kropp, E. M., Chuppa, S. L., Kwok, W.-M., Wu, J. C., … Gundry, R. L. (2014a). High efficiency differentiation of human pluripotent stem cells to cardiomyocytes and characterization by flow cytometry. Journal of Visualized Experiments: JoVE, (91), 52010. https://doi.org/10.3791/52010

Burridge, P. W., Matsa, E., Shukla, P., Lin, Z. C., Churko, J. M., Ebert, A. D., … Wu, J. C. (2014). Chemically defined generation of human cardiomyocytes. Nature Methods, 11(8), 855–860. https://doi.org/10.1038/nmeth.2999

Capell, B. C., Tlougan, B. E., & Orlow, S. J. (2009). From the rarest to the most common: insights from progeroid syndromes into skin cancer and aging. The Journal of Investigative Dermatology, 129(10), 2340–2350. https://doi.org/10.1038/jid.2009.103

Catt, K. J., Cain, M. D., Zimmet, P. Z., & Cran, E. (1969). Blood angiotensin II levels of normal and hypertensive subjects. British Medical Journal, 1(5647), 819–821.

Cox, D. B. T., Platt, R. J., & Zhang, F. (2015). Therapeutic genome editing: prospects and challenges. Nature Medicine, 21(2), 121–131. https://doi.org/10.1038/nm.3793

Crispr Genome Editing, Cas9 Crispr | TransOMIC. (n.d.). Retrieved February 26, 2017, from http://www.transomic.com/Products/CRISPR-Genome-Editing.aspx#1196d0f7-2c89-4fc0-9f4d-ed02072b5bb8,6689105

Cyranoski, D. (n.d.). Japanese woman is first recipient of next-generation stem cells. Nature News. https://doi.org/10.1038/nature.2014.15915

Dubois, N. C., Craft, A. M., Sharma, P., Elliott, D. A., Stanley, E. G., Elefanty, A. G., … Keller, G. (2011). SIRPA is a specific cell-surface marker for isolating cardiomyocytes derived from human pluripotent stem cells. Nature Biotechnology, 29(11), 1011–1018. https://doi.org/10.1038/nbt.2005

Eguchi, T., & Kuboki, T. (2016). Cellular Reprogramming Using Defined Factors and MicroRNAs. Stem Cells International, 2016, e7530942. https://doi.org/10.1155/2016/7530942

Eriksson, M., Brown, W. T., Gordon, L. B., Glynn, M. W., Singer, J., Scott, L., … Collins, F. S. (2003). Recurrent de novo point mutations in lamin A cause Hutchinson-Gilford progeria syndrome. Nature, 423(6937), 293–298. https://doi.org/10.1038/nature01629

Fonoudi, H., Ansari, H., Abbasalizadeh, S., Blue, G. M., Aghdami, N., Winlaw, D. S., … Baharvand, H. (2016). Large-Scale Production of Cardiomyocytes from Human Pluripotent Stem Cells Using a Highly Reproducible Small Molecule-Based Differentiation Protocol. Journal of Visualized Experiments: JoVE, (113). https://doi.org/10.3791/54276

Fu, Y., Sander, J. D., Reyon, D., Cascio, V. M., & Joung, J. K. (2014). Improving CRISPR-Cas nuclease specificity using truncated guide RNAs. Nature Biotechnology, 32(3), 279–284. https://doi.org/10.1038/nbt.2808

Gaj, T., Gersbach, C. A., & Barbas, C. F. (2013). ZFN, TALEN, and CRISPR/Cas-based methods for genome engineering. Trends in Biotechnology, 31(7), 397–405. https://doi.org/10.1016/j.tibtech.2013.04.004

Gordon, L. B., Harten, I. A., Patti, M. E., & Lichtenstein, A. H. (2005). Reduced adiponectin and HDL cholesterol without elevated C-reactive protein: clues to the biology of premature atherosclerosis in Hutchinson-Gilford Progeria Syndrome. The Journal of Pediatrics, 146(3), 336–341. https://doi.org/10.1016/j.jpeds.2004.10.064

Hendriks, W. T., Jiang, X., Daheron, L., & Cowan, C. A. (2015). TALEN- and CRISPR/Cas9-Mediated Gene Editing in Human Pluripotent Stem Cells Using Lipid-Based Transfection. Current Protocols in Stem Cell Biology, 34, 5B.3.1-25. https://doi.org/10.1002/9780470151808.sc05b03s34

Hendriks, W. T., Warren, C. R., & Cowan, C. A. (2016). Genome Editing in Human Pluripotent Stem Cells: Approaches, Pitfalls, and Solutions. Cell Stem Cell, 18(1), 53–65. https://doi.org/10.1016/j.stem.2015.12.002

Horton, J. D., Goldstein, J. L., & Brown, M. S. (2002). SREBPs: activators of the complete program of cholesterol and fatty acid synthesis in the liver. The Journal of Clinical Investigation, 109(9), 1125–1131. https://doi.org/10.1172/JCI15593

Hotta, A., & Yamanaka, S. (2015a). From Genomics to Gene Therapy: Induced Pluripotent Stem Cells Meet Genome Editing. Annual Review of Genetics, 49, 47–70. https://doi.org/10.1146/annurev-genet-112414-054926

iPS cells and reprogramming: turn any cell of the body into a stem cell | Eurostemcell. (n.d.). Retrieved February 26, 2017, from http://www.eurostemcell.org/ips-cells-and-reprogramming-turn-any-cell-body-stem-cell

Ishikawa, S., Kuno, A., Tanno, M., Miki, T., Kouzu, H., Itoh, T., … Miura, T. (2012). Role of connexin-43 in protective PI3K-Akt-GSK-3β signaling in cardiomyocytes. American Journal of Physiology. Heart and Circulatory Physiology, 302(12), H2536-2544. https://doi.org/10.1152/ajpheart.00940.2011

Joung, J. K., & Sander, J. D. (2013a). TALENs: a widely applicable technology for targeted genome editing. Nature Reviews. Molecular Cell Biology, 14(1), 49–55. https://doi.org/10.1038/nrm3486

Kehat, I., Kenyagin-Karsenti, D., Snir, M., Segev, H., Amit, M., Gepstein, A., … Gepstein, L. (2001a). Human embryonic stem cells can differentiate into myocytes with structural and functional properties of cardiomyocytes. Journal of Clinical Investigation, 108(3), 407–414.

Kehat, I., Kenyagin-Karsenti, D., Snir, M., Segev, H., Amit, M., Gepstein, A., … Gepstein, L. (2001b). Human embryonic stem cells can differentiate into myocytes with structural and functional properties of cardiomyocytes. Journal of Clinical Investigation, 108(3), 407–414.

Lian, X., Hsiao, C., Wilson, G., Zhu, K., Hazeltine, L. B., Azarin, S. M., … Palecek, S. P. (2012). Robust cardiomyocyte differentiation from human pluripotent stem cells via temporal modulation of canonical Wnt signaling. Proceedings of the National Academy of Sciences of the United States of America, 109(27), E1848-1857. https://doi.org/10.1073/pnas.1200250109

Liu, G.-H., Barkho, B. Z., Ruiz, S., Diep, D., Qu, J., Yang, S.-L., … Izpisua Belmonte, J. C. (2011). Recapitulation of premature ageing with iPSCs from Hutchinson-Gilford progeria syndrome. Nature, 472(7342), 221–225. https://doi.org/10.1038/nature09879

Mali, P., Esvelt, K. M., & Church, G. M. (2013). Cas9 as a versatile tool for engineering biology. Nature Methods, 10(10), 957–963. https://doi.org/10.1038/nmeth.2649

Marraffini, L. A. (2016). The CRISPR-Cas system of Streptococcus pyogenes: function and applications. In J. J. Ferretti, D. L. Stevens, & V. A. Fischetti (Eds.),

Streptococcus pyogenes: Basic Biology to Clinical Manifestations. Oklahoma City (OK): University of Oklahoma Health Sciences Center. Retrieved from http://www.ncbi.nlm.nih.gov/books/NBK355562/

Nakanishi, M., & Otsu, M. (2012). Development of Sendai Virus Vectors and their Potential Applications in Gene Therapy and Regenerative Medicine. Current Gene Therapy, 12(5), 410–416. https://doi.org/10.2174/156652312802762518

nbt.3070.pdf. (n.d.). Retrieved from http://www.nature.com.ezp-prod1.hul.harvard.edu/nbt/journal/v33/n1/pdf/nbt.3070.pdf

Oudit, G. Y., Crackower, M. A., Backx, P. H., & Penninger, J. M. (2003). The role of ACE2 in cardiovascular physiology. Trends in Cardiovascular Medicine, 13(3), 93–101.

Pagliuca, F. W., Millman, J. R., Gürtler, M., Segel, M., Van Dervort, A., Ryu, J. H., … Melton, D. A. (2014). Generation of functional human pancreatic β cells in vitro. Cell, 159(2), 428–439. https://doi.org/10.1016/j.cell.2014.09.040

Paige, S. L., Plonowska, K., Xu, A., & Wu, S. M. (2015). Molecular Regulation of Cardiomyocyte Differentiation. Circulation Research, 116(2), 341–353. https://doi.org/10.1161/CIRCRESAHA.116.302752

Peters, D. T., Henderson, C. A., Warren, C. R., Friesen, M., Xia, F., Becker, C. E., … Cowan, C. A. (2016). Asialoglycoprotein receptor 1 is a specific cell-surface marker for isolating hepatocytes derived from human pluripotent stem cells. Development (Cambridge, England), 143(9), 1475–1481. https://doi.org/10.1242/dev.132209

Poleganov, M. A., Eminli, S., Beissert, T., Herz, S., Moon, J.-I., Goldmann, J., … Sahin, U. (2015). Efficient Reprogramming of Human Fibroblasts and Blood-Derived Endothelial Progenitor Cells Using Nonmodified RNA for Reprogramming and Immune Evasion. Human Gene Therapy, 26(11), 751–766. https://doi.org/10.1089/hum.2015.045

Sagelius, H., Rosengardten, Y., Schmidt, E., Sonnabend, C., Rozell, B., & Eriksson, M. (2008). Reversible phenotype in a mouse model of Hutchinson-Gilford progeria syndrome. Journal of Medical Genetics, 45(12), 794–801. https://doi.org/10.1136/jmg.2008.060772

Sander, J. D., & Joung, J. K. (2014a). CRISPR-Cas systems for editing, regulating and targeting genomes. Nature Biotechnology, 32(4), 347–355. https://doi.org/10.1038/nbt.2842

Scaffidi, P., & Misteli, T. (2006). Lamin A-dependent nuclear defects in human aging. Science (New York, N.Y.), 312(5776), 1059–1063. https://doi.org/10.1126/science.1127168

Schlaeger, T. M., Daheron, L., Brickler, T. R., Entwisle, S., Chan, K., Cianci, A., … Daley, G. Q. (2015a). A comparison of non-integrating reprogramming methods. Nature Biotechnology, 33(1), 58–63. https://doi.org/10.1038/nbt.3070

Siller, R., Greenhough, S., Naumovska, E., & Sullivan, G. J. (2015). Small-molecule-driven hepatocyte differentiation of human pluripotent stem cells. Stem Cell Reports, 4(5), 939–952. https://doi.org/10.1016/j.stemcr.2015.04.001

Siu, C.-W., Lee, Y.-K., Ho, J. C.-Y., Lai, W.-H., Chan, Y.-C., Ng, K.-M., … Tse, H.-F. (2012a). Modeling of lamin A/C mutation premature cardiac aging using patient−specific induced pluripotent stem cells. Aging, 4(11), 803–822. https://doi.org/10.18632/aging.100503

Sonkusare, S., Palade, P. T., Marsh, J. D., Telemaque, S., Pesic, A., & Rusch, N. J. (2006). Vascular calcium channels and high blood pressure: pathophysiology and therapeutic implications. Vascular Pharmacology, 44(3), 131–142. https://doi.org/10.1016/j.vph.2005.10.005

Strandgren, C., Nasser, H. A., McKenna, T., Koskela, A., Tuukkanen, J., Ohlsson, C., … Eriksson, M. (2015). Transgene silencing of the Hutchinson-Gilford progeria syndrome mutation results in a reversible bone phenotype, whereas resveratrol treatment does not show overall beneficial effects. FASEB Journal: Official Publication of the Federation of American Societies for Experimental Biology, 29(8), 3193–3205. https://doi.org/10.1096/fj.14-269217

Takahashi, K., & Yamanaka, S. (2006). Induction of pluripotent stem cells from mouse embryonic and adult fibroblast cultures by defined factors. Cell, 126(4), 663–676. https://doi.org/10.1016/j.cell.2006.07.024

Takeda, T., & Kohno, M. (1995). Brain natriuretic peptide in hypertension. Hypertension Research: Official Journal of the Japanese Society of Hypertension, 18(4), 259–266.

Tzahor, E. (2007). Wnt/beta-catenin signaling and cardiogenesis: timing does matter. Developmental Cell, 13(1), 10–13. https://doi.org/10.1016/j.devcel.2007.06.006

Ullrich, N. J., & Gordon, L. B. (2015). Hutchinson-Gilford progeria syndrome. Handbook of Clinical Neurology, 132, 249–264. https://doi.org/10.1016/B978-0-444-62702-5.00018-4

Urnov, F. D., Rebar, E. J., Holmes, M. C., Zhang, H. S., & Gregory, P. D. (2010). Genome editing with engineered zinc finger nucleases. Nature Reviews. Genetics, 11(9), 636–646. https://doi.org/10.1038/nrg2842

Vasiliou, S. K., Diamandis, E. P., Church, G. M., Greely, H. T., Baylis, F., Thompson, C., & Schmitt-Ulms, G. (2016). CRISPR-Cas9 System: Opportunities and Concerns. Clinical Chemistry, 62(10), 1304–1311. https://doi.org/10.1373/clinchem.2016.263186

Wong, N. S., & Morse, M. A. (2012). Lonafarnib for cancer and progeria. Expert Opinion on Investigational Drugs, 21(7), 1043–1055. https://doi.org/10.1517/13543784.2012.688950

Yamanaka, S. (2009). A fresh look at iPS cells. Cell, 137(1), 13–17. https://doi.org/10.1016/j.cell.2009.03.034

Yu, C., Liu, Y., Ma, T., Liu, K., Xu, S., Zhang, Y., … Qi, L. S. (2015). Small molecules enhance CRISPR genome editing in pluripotent stem cells. Cell Stem Cell, 16(2), 142–147. https://doi.org/10.1016/j.stem.2015.01.003

Zhang, J., Lian, Q., Zhu, G., Zhou, F., Sui, L., Tan, C., … Colman, A. (2011). A human iPSC model of Hutchinson Gilford Progeria reveals vascular smooth muscle and mesenchymal stem cell defects. Cell Stem Cell, 8(1), 31–45. https://doi.org/10.1016/j.stem.2010.12.002